Advances in Unsaturated Soils

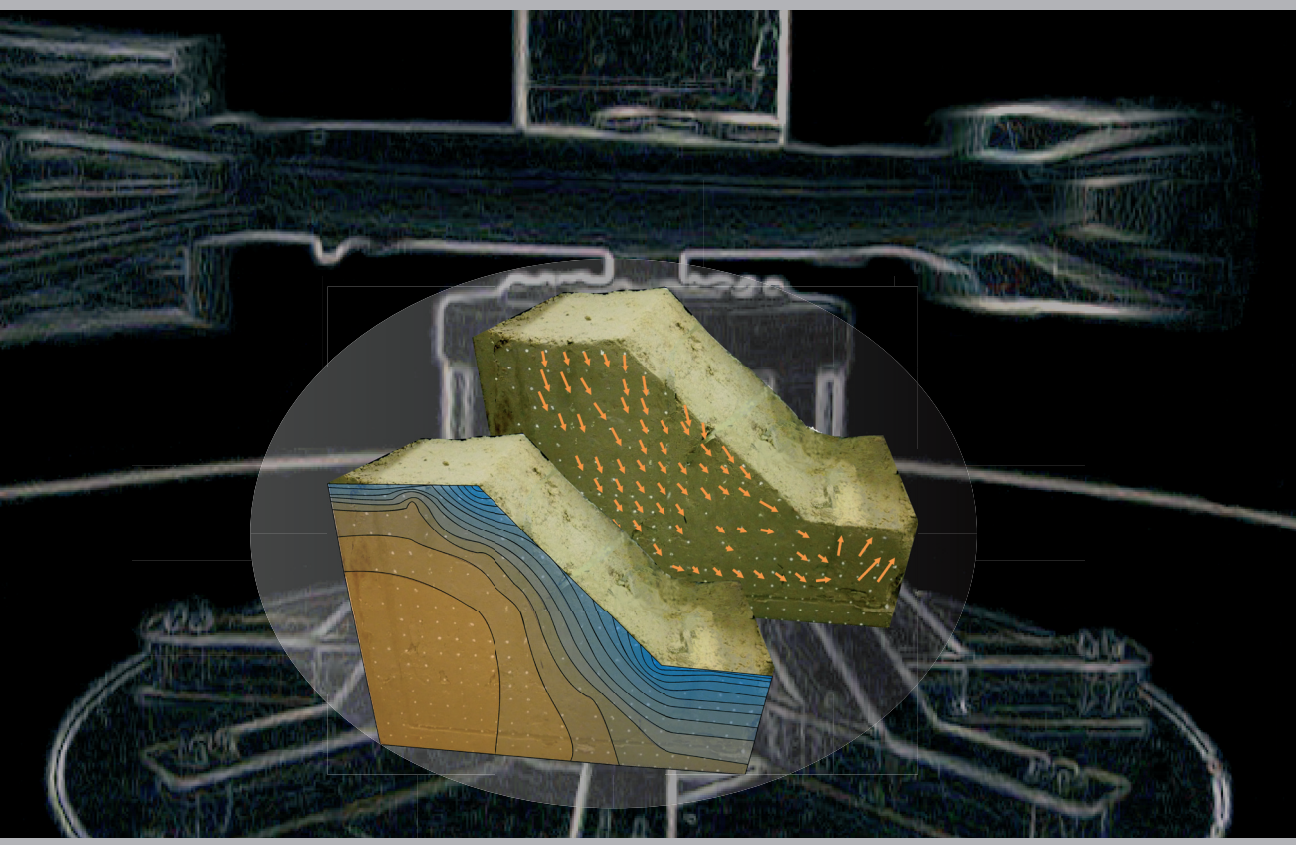

Editor:
Bernardo Caicedo

Co-editors:
Carol Murillo, Laureano Hoyos, Julio E. Colmenares & Iván R. Berdugo

CRC Press
Taylor & Francis Group
A BALKEMA BOOK

ADVANCES IN UNSATURATED SOILS

This page intentionally left blank

PROCEEDINGS OF THE FIRST PAN-AMERICAN CONFERENCE ON UNSATURATED SOILS, CARTAGENA DE INDIAS, COLOMBIA, 20–22 FEBRUARY 2013

Advances in Unsaturated Soils

Editor

Bernardo Caicedo
Department of Civil and Environmental Engineering, Universidad de Los Andes, Bogotá, Colombia

Co-editors

Carol Murillo
Department of Civil and Agricultural Engineering, Universidad Nacional de Colombia, Bogotá, Colombia

Laureano Hoyos
Department of Civil Engineering, The University of Texas at Arlington, USA

Julio Esteban Colmenares
Department of Civil and Agricultural Engineering, Universidad Nacional de Colombia, Bogotá, Colombia

Iván Rafael Berdugo
Department of Civil and Environmental Engineering, Universidad del Norte, Barranquilla, Colombia

CRC Press
Taylor & Francis Group
Boca Raton London New York Leiden

CRC Press is an imprint of the
Taylor & Francis Group, an **informa** business

A BALKEMA BOOK

CRC Press
Taylor & Francis Group
6000 Broken Sound Parkway NW, Suite 300
Boca Raton, FL 33487-2742

Version Date: 20130411

International Standard Book Number-13: 978-0-203-77107-5 (eBook - PDF)

Advances in Unsaturated Soils – Caicedo et al. (eds)
© 2013 Taylor & Francis Group, London, ISBN 978-0-415-62095-6

Table of contents

Numerical modelling

Geotechnical problems and soil atmosphere interaction

This page intentionally left blank

Advances in Unsaturated Soils – Caicedo et al. (eds)
© 2013 Taylor & Francis Group, London, ISBN 978-0-415-62095-6

Preface

There are two main factors explaining the increased interest for Unsaturated Soils in recent years. The first factor is the enhancement of the domain of application of the new theories developed for Unsaturated Soils, which nowadays includes materials like rocks, rock fills, frozen soils and domiciliary solid wastes; and, the efficient applicability of these theories to study new energy-related problems like CO_2 sequestration and nuclear waste disposal, among others. The second factor is the appearance of new experimental techniques that has permitted the analysis of several traditional problems from a new perspective (e.g., swelling or collapsible soils and compacted soils or pavements materials, among others).

In the Americas, the study of unsaturated soils has received particular attention since the apparition of the first theories explaining the behavior of expansive soils. Besides, the recently developed theories constitute effective tools to study the complexity of soils present in the continent, such as residual soils, expansive and collapsing soils and mud rocks, and its interaction with extreme climatic variations.

Advances in Unsaturated Soils is the result of the 1st Pan-American Conference on Unsaturated Soils organized in Cartagena de Indias, Colombia, in February 2013 by Los Andes University and the Colombian National University (Bogotá). The book contains a compendium of the works presented in the conference, and it represents a stimulating sample of every aspect included in the study of unsaturated soils up to 2013. Besides, it links together fundamental knowledge, testing techniques, computational procedures and prediction methodologies. The volume includes 76 research papers coming for all over the world, as well as 7 keynotes papers from international researchers.

I am grateful for the keynote papers prepared by professors Eduardo Alonso, Geoffrey Blight, Delwyn Fredlund, Antonio Gens, Sandra Houston, Serge Leroueil, Robert Lytton, Luciano Oldecop and Sai Vanapalli, and their co-authors. Certainly, these keynotes will become reference papers for researchers and practitioners interested in the area of unsaturated soils.

I would also like to express our gratitude to the international committee TC106 of the International Society for Soil Mechanics and Geotechnical Engineering, who supported this conference, as well as to our co-sponsors: the University of Texas at Arlington, and the Geo Institute.

Finally, thanks are due to all the authors who submitted papers to the conference, to the reviewers who offered an essential part of their time to enhance the quality of these contributions, and to the local organizing committee and the international advisory board for their continuous support.

I hope that this volume will inspire future generations involved in geotechnical engineering of unsaturated soils.

Bernardo Caicedo
Chair, First Pan-American Conference on Unsaturated Soils

This page intentionally left blank

Advances in Unsaturated Soils – Caicedo et al. (eds)
© 2013 Taylor & Francis Group, London, ISBN 978-0-415-62095-6

Organization committees

LOCAL ORGANIZING COMMITTEE

Bernardo Caicedo, *Los Andes University, Colombia*
Manuel García, *National University of Colombia, Bogotá*
Silvia Caro, *Los Andes University, Colombia*
Iván Rafael Berdugo, *Universidad del Norte, Barranquilla*
Julio Esteban Colmenares, *National University of Colombia, Bogotá*
Nicolás Estrada, *Los Andes University, Colombia*
Laureano Hoyos, *University of Texas, Arlington, USA*
Arcesio Lizcano, *Los Andes University, Colombia*
Carol Murillo, *National University of Colombia, Bogotá*

ORGANIZER COORDINATOR

Diana Bolena Sánchez

INTERNATIONAL ADVISORY BOARD

E. Alonso (Spain)
J.L. Briaud (USA)
P. Delage (France)
D. Gallipoli (United Kingdom)
G. Gitirana (Brazil)
S. Houston (USA)
C. Jommi (Italy)
L. Laloui (Switzerland)
W. Likos (USA)
N. Lu (USA)
D. Marcial (Venezuela)
J.S. McCartney (USA)
L. Oldecop (Argentina)
M. Pérez (Mexico)
E. Rojas (México)
M. Sánchez (USA)
A. Tarantino (United Kingdom)
S. Vanapalli (Canada)
A. Zepeda (Mexico)
K. Bicalho (Brazil)
T.M. Pereira de Campos (Brazil)
D. Fredlund (Canada)
A. Gens (Spain)
L. Guimaraes (Brazil)
D. Hurtado (Mexico)
J.F. Thomé Jucá (Brazil)
S. Leroueil (Canada)
T. López (Mexico)
R. Lytton (USA)
F. Marinho (Brazil)
F. Masrouri (France)
A. Pérez (Mexico)
A. Puppala (USA)
E. Romero (Spain)
S. Springman (Switzerland)
L. Vallejo (USA)
O. Monje (Brazil)

This page intentionally left blank

Advances in Unsaturated Soils – Caicedo et al. (eds)
© 2013 Taylor & Francis Group, London, ISBN 978-0-415-62095-6

Acknowledgements

MANUSCRIPT REVIEWERS

The editors are grateful to the following people who helped to review the manuscripts and hence assisted in improving the overall technical standard and presentation of the papers in these proceedings:

J.P. Alvarado
K. Bicalho
D. Cantor
D. Castillo
D. Gallipoli
L. Garzón
G. Gitirana
D. Gómez
L. Guimaraes
D. Marcial
F. Marinho
F. Masrouri
J.S. McCartney
J. Miller
J. Muñoz
F. Lopez
C. Lozada
N. Lu
M. Ocampo
L. Oldecop
T.M Pereira de Campos
L. Ramirez
D. Rojas
E. Rueda
D.B. Sánchez
M. Sánchez
A. Tarantino
J.F. Thomé
L. Thorel
D. Toll
L. Vallejo
S. Vanapalli
L.F. Vesga
C.E. Zapata

This page intentionally left blank

Advances in Unsaturated Soils – Caicedo et al. (eds)
© 2013 Taylor & Francis Group, London, ISBN 978-0-415-62095-6

Sponsors

First Pan-American Conference on
Unsaturated Soils

HOSTING ORGANIZATIONS

Universidad de los Andes

UNIVERSIDAD NACIONAL DE COLOMBIA
SEDE BOGOTÁ
FACULTAD DE INGENIERÍA

CO-SPONSORS

UNIVERSITY OF TEXAS ARLINGTON

ISSMGE

G-I GEO-INSTITUTE
ASCE

ceiBA

This page intentionally left blank

Keynotes lectures

This page intentionally left blank

Advances in Unsaturated Soils – Caicedo et al. (eds)
© 2013 Taylor & Francis Group, London, ISBN 978-0-415-62095-6

Interactions between atmosphere and geosphere—difficulties in measuring evaporation

Geoffrey Blight
University of the Witwatersrand, Johannesburg, South Africa

ABSTRACT: The solar energy balance method and semi-empirical derivatives of this approach are widely used to estimate evaporation (or evapotranspiration) from the soil-covered or soil-like surfaces of waste storage facilities, in order to evaluate the water balances for the facilities. A number of difficulties and uncertainties regarding evaluation of the solar energy balance have been experienced. This paper gives six examples of these, with the purpose of warning against the incautious use of the method.

1 INTRODUCTION

Assessment of the water balance is an essential step in the design of any municipal solid, industrial or mine waste storage facility. The water balance calculation enables the designer to estimate the quantities of water entering, retained within and exiting the waste body (e.g., Fenn, et al., 1975, Blight, 2010 and others). The inputs to the landfill or other waste storage facility usually consist of the water content of the incoming waste and the rainfall infiltration for the site, and the outputs are evaporation from the surface and leachate or seepage exiting from the base of the deposit. Estimation of the inputs and the output evaporation enables the quantity of leachate or seepage to be predicted. This in turn allows the need for an impervious underliner, to prevent ground-water contamination, to be assessed as well as the quantities of leachate or seepage for which the drainage or seepage effluent treatment system need to be designed. Fluctuating water storage within the waste body bridges between inputs and outputs and completes the water balance. At closure of the storage facility, the water balance needs to be reassessed for post-closure conditions to decide on the need for ongoing leachate collection, storage and treatment and to design the post-closure facilities. Recently, Henken-Mellies and Schweizer, (2011) have emphasized the ongoing importance of water balance estimation in all phases of the life-cycles of waste storage facilities.

Evaporation almost always represents a major term in the water balance equation and is also one of the most difficult to quantify. During the 1960s to 1990s, the fields of plant physiology, forestry and agriculture formalized a means of estimating evaporation from soil and water surfaces, based on the solar energy balance (Penman, 1956, Monteith, 1980, Calder, 1990).

However, there are several difficulties in applying the solar energy method to the calculation of water balances in the field of waste storage. Some of these were enumerated and analysed by Blight (2009, 2010). The purpose of this paper is to describe these problems, in order to warn of their existence. Their solution is not clear, as yet, but forewarned is forearmed, and knowing of their existence can prevent the geotechnical engineer working in the waste storage field from making incorrect decisions based on inadequate information.

2 ESTIMATING EVAPOTRANSPIRATION BY SOLAR ENERGY BALANCE

According to established and generally accepted theory, the daily quantity of evaporation or evapotranspiration can be determined by measuring the components of the solar energy balance equation (e.g., Penman, 1963, Monteith, 1980, Calder, 1990) written as:

$$LE = R_n + WE - (G + H + p) \quad (1)$$

The terms are usually expressed in energy units of kJ/m^2, and LE is the latent heat consumed in evaporation or evapotranspiration, R_n is the net incoming short wave solar energy (gross incoming—reflected) at the soil surface, WE is the wind energy (which will not be considered here), G is the energy absorbed by heating the near-surface soil and soil-water (the soil heat), H is the energy absorbed by heating the near-surface air (the sensible heat) and p is the energy used in plant photosynthesis (usually less than 2% of R_n).

LE (in kJ/m^2) is used to calculate the quantity of daily evapotranspiration by dividing the daily total LE by the latent heat for vaporization of water, λ in kJ/kg. That is, evapotranspiration E = LE/λ in kg/m^2. (1 kg/m^2 is equivalent to 1 mm depth of water.) For reasons of lack of space, the reader is referred to Blight (2009 & 2010) for numerical constants and methods of calculating the various terms in equation (1).

In terms of equation (1), G, H and p are heat losses or sinks that subtract from LE and therefore reduce evaporation. One of the problems associated with equation (1) is that it includes only the net incoming short wave-length solar radiation R_n, but omits the outgoing long wave-length Earth heat radiation R_o. This could be subtracted as a proportion (about 25%) of R_n, but because the rate of outgoing heat energy varies throughout the day and night and can be affected by local weather conditions, short-term fluctuations will arise (energy deficits or surpluses) that need to be represented by an energy storage term S, which may be positive or negative (Oke, 1978). With these additions, equation (1) becomes

$$LE = (R_n - R_o) + WE - (G + H + p) + S \qquad (1a)$$

The value of H is negligible in comparison with G and p is also small. The equation lacks a term representing inefficiencies or losses in energy conversion (L). With this addition, equation (1a) can be replaced by

$$LE = (R_n - R_o) + WE - (G + L) + S \qquad (1b)$$

Penman (1956) introduced a semi-empirical equation for calculating evaporation that does not use the energy balance directly, but is based on energy balance principles. His equation is

$$E_p = (\Delta R_n/\lambda + \gamma E_a)/(\Delta + \gamma) \qquad (2)$$

in which E_p is the potential evaporation, Δ is the slope of the temperature versus saturated water vapour pressure curve at the prevailing air temperature, R_n is the net incoming solar radiation, λ is the latent heat for vaporization of water, γ is the psychrometric constant (66 Pa/^{o}C), $E_a = 0.165\,(e_{sat} - e_a)\,(0.8 + u_2/100)$ mm/day, e_{sat} is the saturated vapour pressure of air (mbar), e_a is the actual vapour pressure of air (mbar) and u_2 is the wind speed at a height of 2 m (km/day). Note that E_a (a linear function of u_2) increases E_p, and that no energy storage term appears. As Δ and γ both have units of Pa/^{o}C, if R_n has units of J/m^2 per day and λ has units of J/kg, the units of E_p are kg/m^2, the equivalent of mm/day of water.

Priestly & Taylor (1972) suggested a modified Penman equation that appeared to fit measured evaporation more closely. Their equation is:

$$E_p = 1.26\Delta/\lambda.(R_n - S)/\Delta + \gamma) \qquad (2a)$$

The effect of wind is ignored, and the heat stored in the water or soil being considered is represented by S, regarded as an energy loss. Various others (e.g., de Bruin & Keijman, 1979), have also suggested slight modifications to fit their local climatic conditions.

The original Penman equation (2) is probably the most frequently used method of calculating evaporation from water or soil surfaces. Penman called E_p the potential evaporation, recognizing that actual evaporation could be more or less than this, depending on local circumstances. As evaporation is very often routinely measured by the standard American 'A' evaporation pan, many attempts have also been made to find modification factors that will convert the easily determined A-pan evaporation (E_A) to actual evaporation from soil or water surfaces. Penman (1956) suggested ratios of E_p/E_A for cropped fields varying from 0.8 for summer to 0.6 for winter in Western Europe. Others (quoted by Fenn, et al., 1975) found values for E_p/E_A varying in the range 0.5–0.9. A recent study of the ratio E_B/E_A made at six landfill sites in South Africa (Blight, 2006), gave a large range of seasonal values varying from 0.1 to 0.75 and average annual values from 0.34 to 0.46 with an overall mean of 0.39. E_B is the evapotranspiration measured by energy balance (equation (1), usually with WE, H and p set to zero). The necessity of adopting these correction factors is recognition that both the A-pan and other evaporation pan methods of measuring evaporation as well as the use of equations (1a) and (2) are problematic.

These so-called "crop" or "lake" factors may seem to be a neat solution to the problem, but as shown by Figure 1, can be wildly inaccurate. Figure 1 (Benli, et al., 2010) shows a correlation between A-pan evaporation and evaporation from cropped soil measured directly by means of large-scale lysimeters. No engineer would be happy to apply a correlation like this in work on which his reputation might depend.

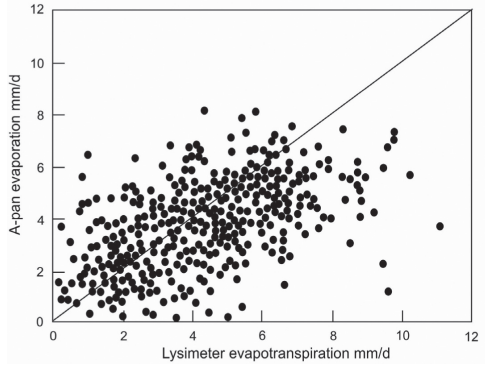

Figure 1. Comparison of two methods of measuring evapotranspiration. (Benli, et al., 2010).

3 DIFFICULTIES IN APPLYING THE ENERGY BALANCE TO ESTIMATING EVAPORATION

3.1 *Field experiments using a large cylindrical pan set into the ground surface (Blight, 2009a)*

Some of the difficulties associated with applying equation (1) are illustrated by Figures 2 and 3. Because similar principles must govern evaporation from both water and soil surfaces, it was decided to pair experiments on water and soil, both to increase understanding of the processes and to act as a series of ongoing checks on the experimental results. A 500 mm diameter by 100 mm deep circular stainless steel pan was let into the surface of a short-mown grassed area so that its rim was level with the soil surface (i.e. slightly below the grass surface). The pan was filled with water and left overnight to reach temperature equilibrium with its surroundings. In the accepted conventional way, the vertical components of the incoming and reflected solar power (in W/m^2) were measured throughout the day, as well as water temperatures. The experiment was then repeated, as a check, a week later. The week thereafter the experiment was carried out with the pan filled with a uniform compacted moist sand. An impervious containing vessel was used so that the depth of water or soil from which water was evaporating could be precisely defined, and at the same time, the sides and base of the soil or water specimen would be insulated by the surrounding soil. The results of the measurements are shown in Figure 2. In the upper diagram, the roughly parabolic curves represent the vertical component of the net incoming solar power $\delta/\delta t R_n(V)$ recorded through the first of each of two test days in W/m^2. The ogive-like curves represent the time-integrated values of $R_n(V)$, in kJ/m^2. The soil heat G is also shown in this diagram. Sunrise was at 07.00 and sunset at 17.00. The lower diagram shows the measured water and soil temperatures, relative to the temperature at sunrise, throughout the day, as well as the residual value at 07.00 the next morning.

The first difficulty that is apparent from Figure 2 is that the maximum soil heat G (5410 kJ/m^2) and water heat WH (8380 kJ/m^2) calculated from the maximum soil and water temperatures exceeded the net cumulative vertical component of solar

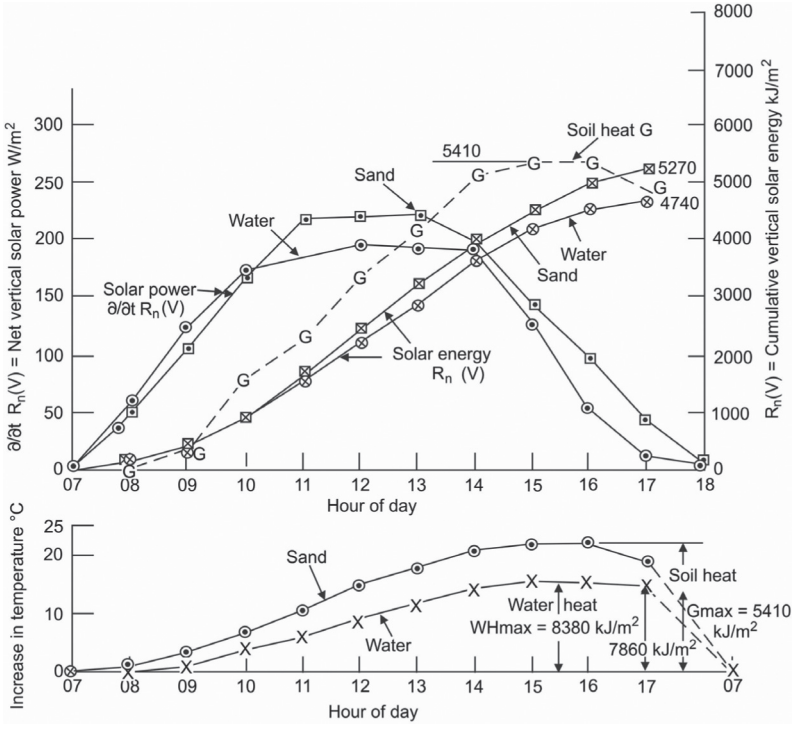

Figure 2. Results of twin experiments made on stainless steel pan set level with ground surface. Pan filled firstly with water, secondly with sand. Measured evaporation (averaged over 5 consecutive days): Water: 3.2 mm/day, Sand: 1.6 mm/day.

energy for the day (of 5270 kJ/m^2 for the sand and 4255 kJ/m^2 for the water). Obviously, more energy was being absorbed by the soil and water than was represented by $R_n(V)$. When the experiment was made with the pan filled with sand, the maximum (R_{max}), the vertical (R_v) and net vertical $R_n(V)$ components of the solar power were measured separately, with the result shown in Figure 3. This shows that the gross incoming solar energy R_{max}, may be 3 times the net value of $R_n(V)$ for the water, which, in conjunction with the completely independently measured G and WH values in Figure 2, must mean that not only the vertical component of solar energy is absorbed at a soil or water surface (as conventionally assumed), but also additional oblique components.

The second difficulty also relates to the values of G. In Figure 2, G exceeded $R_n(V)$ from 09.00 until nearly 16.00. If G is interpreted as a loss and as subtractive from $R_n(V)$, equation (1) would predict negligible evaporation for the day, whereas the actual evaporation measured over 5 days by means of the water contents of cores of sand taken from the pan averaged 1.6 mm/day. Similar results were observed for the evaporation of water (3.2 mm/day).

These tests were repeated several times, varying the colour of the pan's interior surface for tests on water and the water content of the sand and with the pan set into the ground and raised above the surface with insulated sides and base. The results

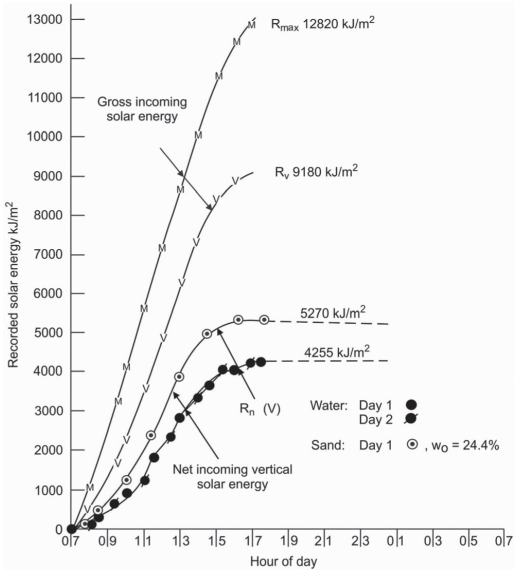

Figure 3. Comparison of gross maximum, vertical and net vertical solar energies. Differences between water and sand for net energies is caused by differences in albedo (reflectance) of surfaces.

were similar in every case. It seemed very likely from the considerations above, that the stored soil and water heat are the opposite of heat losses that decrease evaporation, they are actually the sources and drivers of evaporation.

3.2 *Field measurement of the water balance for a landfill*

Figure 4 shows the water balance, measured over a five year period, for an experimental raising of a landfill in Cape Town, South Africa. (Blight, 2005). In Figure 4, the precipitation, P and the leachate L were measured directly on the landfill, while the evaporation from the landfill surface E_B, was calculated by means of the solar energy balance (eqn. 1). It will be noted from Figure 4 that E_B was by far the largest quantity in the water balance, with an average value of 620 mm/y. The broken line marked E(av) = 400 mm/y shows that there was considerable doubt as to whether the value of 620 mm/y could be correct, as it far exceeded the average annual precipitation of about 400 mm/y, over the 5 year period. Evaporation as large as this would have severely depleted the water stored in the waste, as shown by the solid line labeled ΔS_w. As the landfill continued to emit leachate at an approximately constant rate (L in Figure 4) throughout the 5 years of the experiment, this was unlikely to have happened and cast doubt on the accuracy of assessing E_B. It appears that in this case, eqn. 1 led to a 50% over-estimate of the actual evaporation from the landfill.

3.3 *Evaporation from experimental landfill capping layers*

Figure 5 shows water balance data for a series of experimental landfill covers (or capping layers) constructed in Johannesburg, South Africa to test the infiltrate, stabilize, evapotranspire concept for landfill capping layers (Blight & Fourie, 2005). In Figure 5, evaporation estimated by solar energy balance (E_B) is also the largest component of the water balance and far exceeded rainfall P. The experimental caps were constructed over geomembrane-lined basins, so that all evaporation must have originated in the soil cover, above the geomembrane. As the inset above the main diagram shows, average evaporation rates measured by changes of water content in the soil cover-layers during dry periods were considerably less than rates established by solar energy balance, again throwing doubt on the reliability of the energy balance method, and resulting in up to a seven-fold (2.1/0.3) over-estimate of actual evaporation from the cover-layers. Similar tests carried out at the same time in Cape Town, indicated similar over-estimates of soil evaporation by applying equation (1).

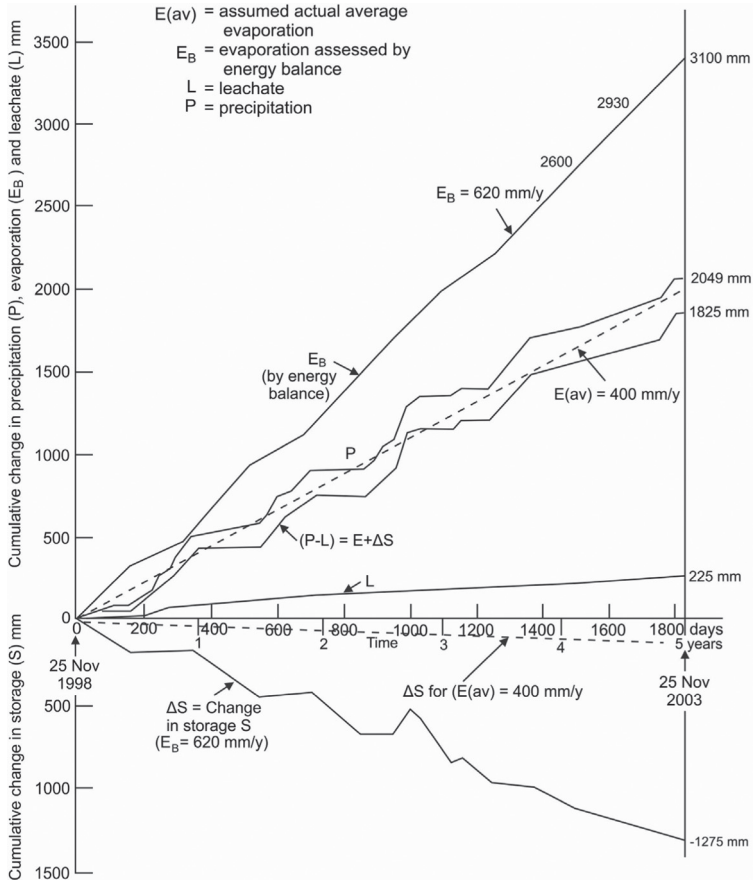

Figure 4. Water balance for raised part of landfill at Cape Town during experiment: changes in water storage as a result of precipitation infiltration, leachate flow and evaporative losses. (November 1998–2003).

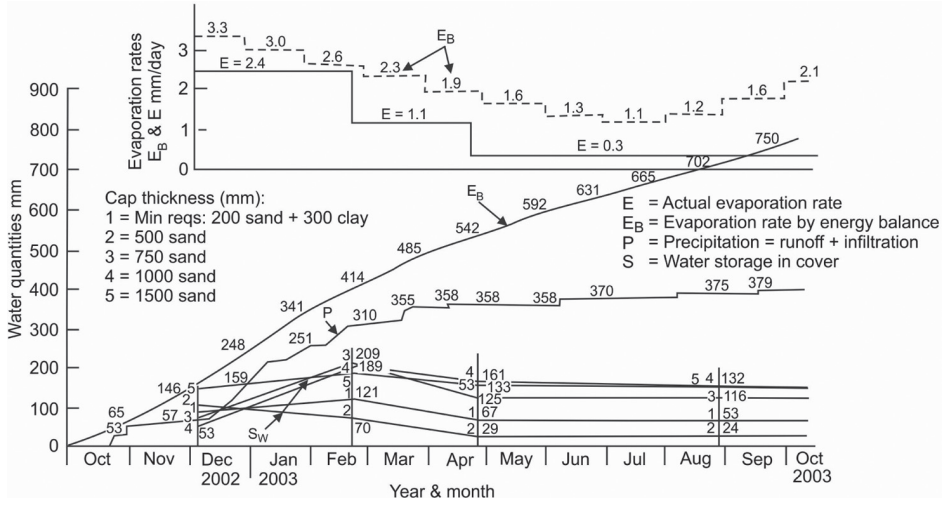

Figure 5. Water balance data for Johannesburg experimental landfill caps: October 2002 to October 2003.

3.4 *Evaporation from a grassed, fissured clay surface*

In the two examples illustrated by Figures 4 and 5, application of equation (1) showed that E_B over-estimated the true evaporation E. In both of these cases, the cover soil was sandy, and apart from any faults with the interpretation of the terms of equation (1), the over-estimate may have been the result of inherent inefficiency in the conversion of stored soil and soil-water heat into evaporation. This has been demonstrated by Blight (2010), pp. 445–446. However, the result of applying equation (1) may in other cases appear accurate or may be an apparent under-estimate of E. Figures 6a and 6b illustrate such cases (Blight, 2006b, 2008a). The soil at the site under consideration consists of 0.5 to 2 m of a stiff fissured clayey silt underlain by sandstone, with the water table at 5 m and a grass-covered surface. Separate studies (Blight, 2009b) had shown that even in rain-storms of as much as 50 mm in 4 hours, run-off from the fissured clay surface was negligible. The measurements for Figure 6a were made under the grassed surface near a lone willow tree. Figure 6a shows the rainfall precipitation (P) and evapotranspiration (EB) for the site from 01 October 2003 to 20 December 2004, with the precipitation measured daily by rain gauge on site, and the evapotranspiration, assessed by equation (1). The water balance for the area adjacent to the lone willow was started in October because it is the end of the dry season and a month in which temperatures are moderate and evapotranspiration low. As Figure 6a shows, in addition to E_B and P, the water stored in the soil profile (S) was measured by means of soil samples taken by hand augering, at 100 mm depth intervals, on six occasions from April to December, 2004. In the case that no water exits the shallow soil profile, to seep down to the water table and no water rises from the water table under a capillary gradient, the following equation should hold:

$$S + E_B = P$$

The inset graph of $(S + E_B)$ against P shows that this was close to true for the data shown on Figure 6a.

The measurements for Figure 6b were made at right angles to a line of evergreen bushes (Leucosidia) and deciduous trees (Populus). Figure 6b shows water balances for the years May 2004 to April 2005 and May 2005 to April 2006, with May to October 2006. The water stored in the soil along two lines at right angles to the line of bushes and trees was measured on two occasions each by hand-augering holes at the positions indicated and measuring water content profiles from surface at intervals of 100 mm down to a depth of 500 mm.

The water stored in the soil remote from the bushes was very similar in quantity on both occasions on which it was sampled and amounted to between 175 and 202 mm. Water stored in the soil remote from the trees amounted to between 152 and 211 mm, i.e. similar to the "bush profiles". By the same argument used above, $(S + E_B)$ should equal P. The experimental points for the assessments of $(S + E_B)$ and P have also been plotted on the graph inset on Figure 6a. These show that as the water stored in the soil decreases, it approaches a constant value as P decreases. This is probably again due to a decreasing efficiency of conversion of soil heat into evaporation, as the surface dries out and surface fissures multiply in number and depth.

An alternate way of looking at the results in Figures 6a and 6b in terms of eqn. (1) is that when the soil is relatively wet, as it was in the measurements in Figure 6a, incoming radiation R_n is almost entirely converted to G, which is then relatively efficiently converted to E. In other words, for a wet soil, eqn. (1b) could be written:

$$LE = R_n + WE = G + WE \tag{1c}$$

As the soil dries out and the energy conversion becomes less efficient, eqn. (1c) would change to

$$LE < G + WE = \eta G + WE \tag{1d}$$

where η is an efficiency factor accounting for inefficiency in conversion of heat energy to evaporation.

This reasoning is illustrated by Figure 7 which shows the results of solar heated evaporation tests similar to those described in Figure 2, but performed on smaller insulated containers so that evaporation could be accurately measured by weighing. The two experimental containers each holding water or a saturated sandy silt, were exposed to the weather at sunset on the day before the tests so that they could equilibrate with ambient conditions. Temperatures of the water and soil were measured by means of thermocouples, and the containers were weighed at intervals throughout the day and the following night.

Figure 7 shows the results plotted in terms of evaporation and stored heat energy (see Blight, 2009). The curves show that as the water or soil heat is absorbed, conversion of heat to evaporation occurred simultaneously. The maximum of stored WH or G occurred at about 15.00, whereafter incident solar radiation decreased rapidly, but conversion of soil heat to evaporation continued. In the early hours of the next morning the heat energy

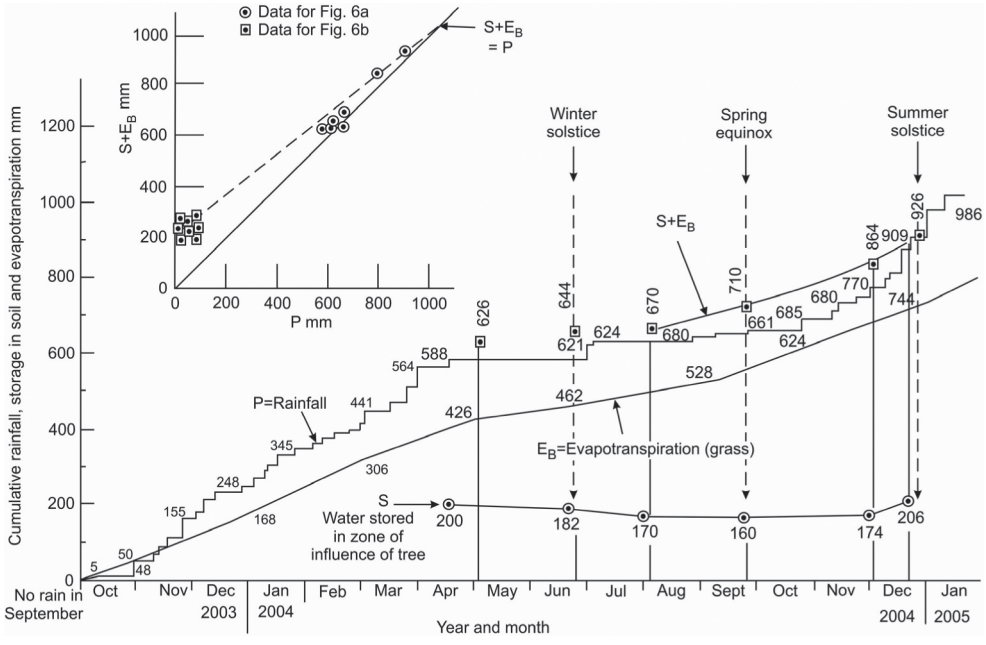

Figure 6a. Water balance data for a grass-covered site adjacent to a single tree where the soil consists of a stiff fissured silty clay of limited thickness, overlying sandstone.

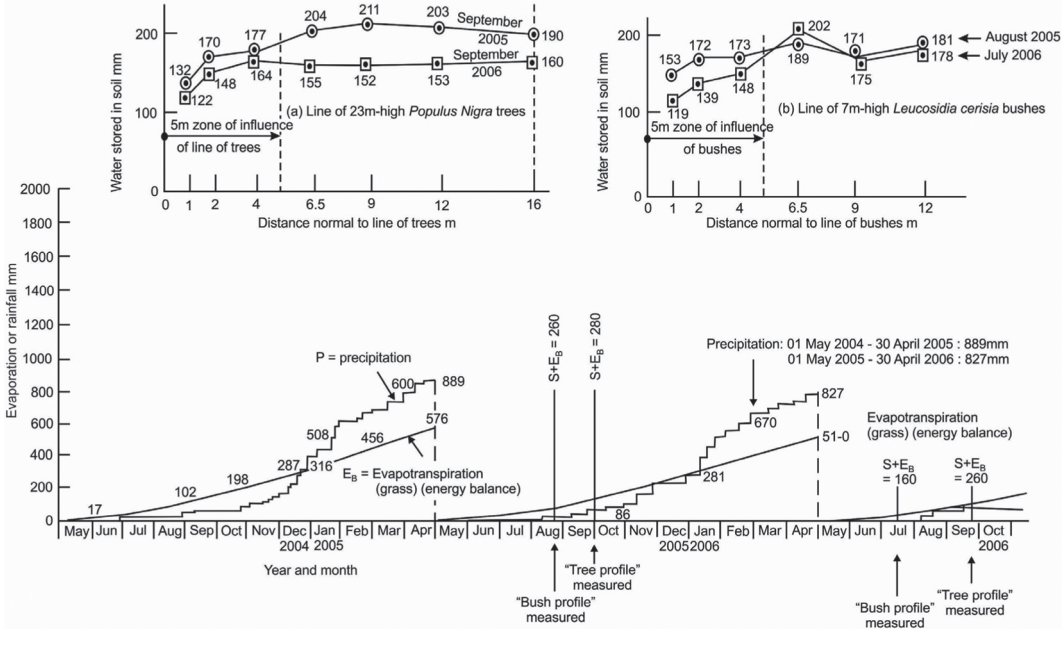

Figure 6b. Water balance for a grass-covered site adjacent to lines of trees and bushes where the soil consists of a stiff fissured silt clay of limited thickness, overlying sandstone.

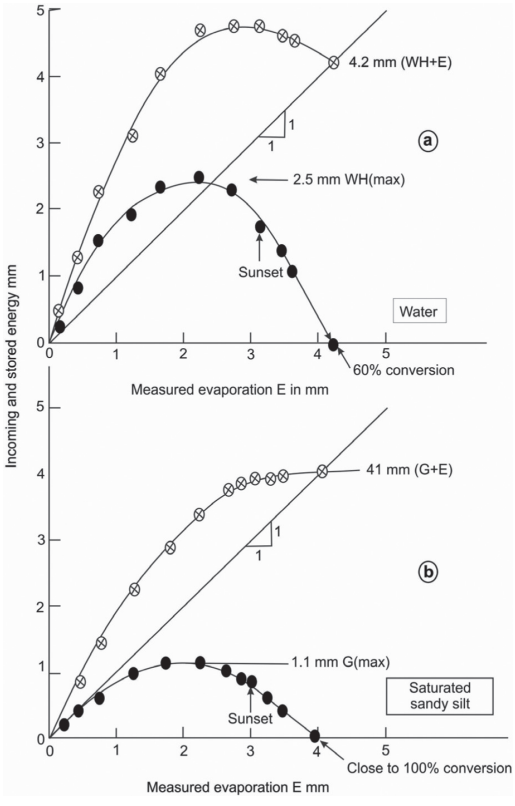

Figure 7. Variation of (a) water and (b) soil heat with evaporation over 24-hour day.

had been exhausted. At this point, evaporation ceased and the sum of the total water or soil heat equaled the evaporation, i.e. in terms of eqn. (1c)

$$LE = WH \text{ or } LE = G$$

3.5 *Near-surface movement of water during evapotranspiration*

The experience described in section 3.4 led to a detailed study of near surface water movement during evapotranspiration (Blight, 2008b). Calibrated glass-fibre mat moisture sensors and gypsum blocks were set and observed in a clayey silt soil beneath a mown grass surface. The observations took place in June, a period with no rain or cloud cover.

Figure 8a shows the decline of water content as evaporation occurred over a period of 16 days at depths of 15, 45 and 75 mm. The gypsum blocks gave very similar results. Figure 8b shows detailed water content profiles measured on days 1 and 8.

While the loss of water over the 8 days from depths 0–75 mm amounted to 0.6 mm/day, that over 0–200 mm amounted to 1.1 mm/day. The latter figure more accurately represents the evapotranspiration from the soil, but the figure is actually larger, as water losses from deeper than 200 mm were not measured. This shows that even direct measurement of evaporation from water content profiles by means of water contents may under-estimate actual evaporation losses.

If it is assumed that the soil heat G at sunset is equivalent to the nocturnal evaporation, a total of 1.6 mm, 0.2 mm/day or roughly 20% of total evaporation took place nocturnally.

3.6 *Drying of tailings beaches*

Apparently anomalous results were observed when studying the rate of drying of 400 mm deep test depositions of platinum tailings on a tailings deposition facility or TSF (Blight, et al., 2012).

To aid in understanding the process of drying of the tailings beaches, a small-scale experiment was set up. A sample of tailings was placed in a small plastic bucket. The bucket was contained in a cardboard box, the base and sides of the bucket being insulated with a minimum of 25 mm of dry wood shavings. The specimen represented a 120 mm thick surface layer of tailings, isolated from interchange of pore water with the tailings around or below it and with the insulation preventing any gain or loss of heat by the tailings specimen, except through the top surface. Changes of mass of the tailings could be measured by weighing to 0.5 g which represented a water loss or gain of 0.03 mm. To record the development of pore water suction in the tailings, two calibrated gypsum block sensors were set into the tailings, one centred 20 mm from the surface and the other at 100 mm below the surface. The bucket of tailings and an identical insulated bucket of water were exposed to the weather, supported 1 m above the ground on a small wooden table, in an area receiving sun from sunrise to sunset. The test was carried out in cool weather during May/June when there was no rain or cloud.

The results of the experiment are shown in Figure 9. Referring to the left diagram, starting at a value of 38.6% the water content declined to 27% after 7 days of exposure before the gypsum blocks registered any suction. As the water content continued to decline, the suction rose by the day, reaching 300 kPa after another 7 days. The important point to note is that suction was only generated once the water content fell below a threshold value (i.e. its field capacity), in this case 27%. Until this threshold was reached, the near-surface pore water was unstressed, and therefore free either to seep downwards into the tailings below, under the gravity pressure gradient, or to be evaporated. The proportions in which these two possible movements occur appears unpredictable.

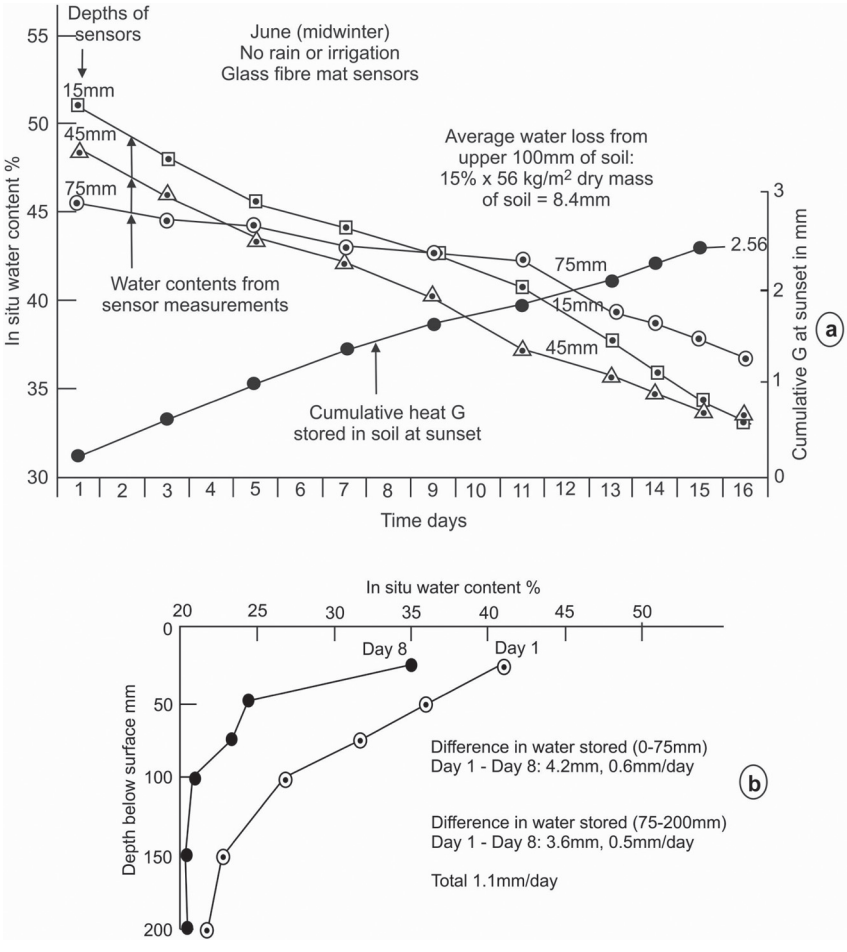

Figure 8. Results of study of near-surface movement of water caused by evaporation.

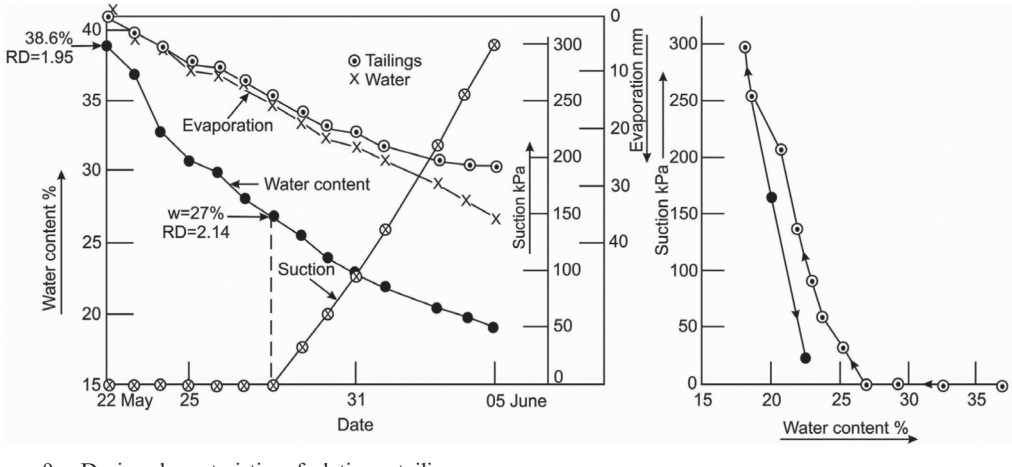

Figure 9. Drying characteristics of platinum tailings.

A suction of 300 kPa represents 30 m of negative water head which is sufficient to draw water up to the tailings surface from a depth of 30 m. It must also be noted that the whole mass of tailings retained by the TSF is consolidating under its own weight. The TSF is built on a highly impervious black clay stratum, for which the permeability, measured in the laboratory, is 0.03 m/y compared with 2 to 3 m/y for the tailings. Although originally desiccated and highly fissured, the clay was presently swollen with seepage water and compressed by the 30 m of overburden imposed by the tailings. Hence, water expelled by consolidation was much more likely to be moving towards the surface of the tailings than towards the impervious foundation stratum.

Calculations based on the consolidation characteristics of the tailings showed that the tailings mass is 90% consolidated and the surface of the tailings is settling at between 1 and 0.1 mm per day depending on the assumptions made. As the porosity of the tailings is about 0.6, 0.6 to 0.06 mm/day of consolidation water is being liberated at the surface. This is enough to partly supply the evaporation during hot weather, and to keep the near-surface tailings damp during cool weather.

The left diagram in Figure 9 shows the cumulative amounts of evaporation of water from both the tailings and water surfaces. Initially, there was very little difference in evaporation losses from the water and tailings surfaces, but once the suction threshold had been passed, evaporation from the tailings slowed, while that from the water surface continued at an almost constant rate. This is mainly because the efficiency of evaporation from the tailings surface reduced considerably as the tailings progressively de-saturated.

The right diagram in Figure 9 shows the suction-water content curve (or SWCC) for the tailings. After the suction reached 300 kPa, the tailings were re-wetted in two stages so as to develop the re-wetting branch of the SWCC. Note that the re-wetting branch is both considerably steeper and, within the suction range of 0–300 kPa, almost completely reversible.

Figure 10 shows typical water content profiles at various times after deposition for two test depositions: (a) and (b). Considering (a), a depth of 400 mm represents the surface of the previous layer, where on 22 March there was evidence that the surface had dried to less than 20% water content.

The water content at this depth did not increase much above this value, because the tailings would now have been on the re-wetting branch of the SWCC (Figure 9, right). It will also be seen that it took 13 to 14 days for the water content at the surface to decrease below 30%, and 28 days after deposition had ceased, the surface water content had only decreased by 6% to 24%, roughly 0.21% per day. Comparing with Figure 9, where the water content reduced by roughly 1.4% per day, in the first 14 days, the drying appears to have been very slow. This is because the surface water content was being augmented continually by water, both evaporation and consolidation water rising from below. This could not happen in the small-scale test, but

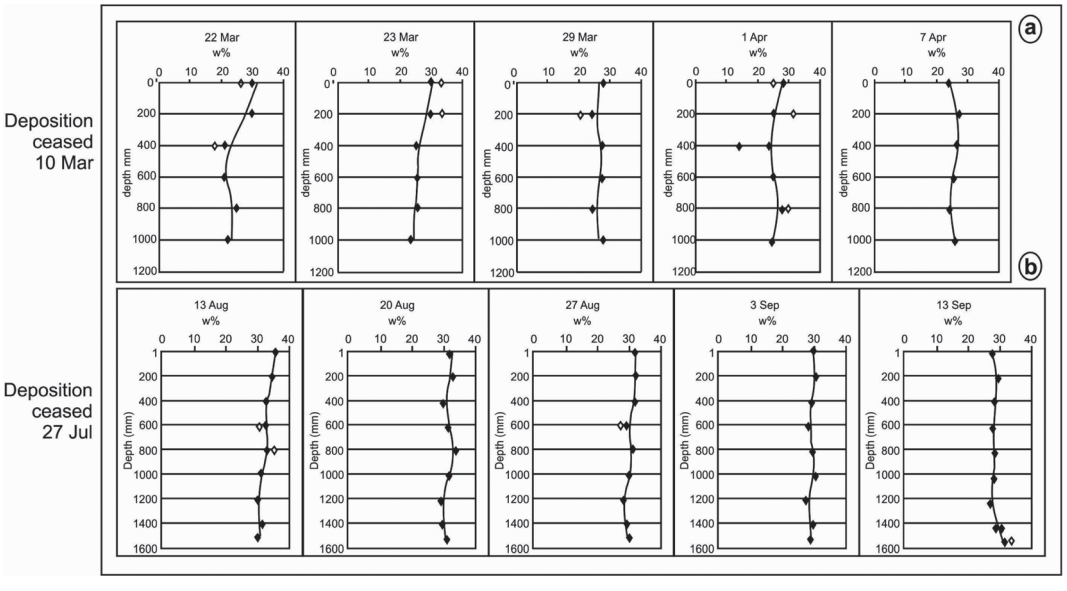

Figure 10. Water content profiles measured at various times in two layers of recently deposited platinum tailings.

the mechanism becomes apparent when the full scale beach is compared with the small-scale test.

Considering Figure 10b, it took 21 days for the surface water content to reduce from 36% to 30%, i.e. 0.29% per day. It is again likely that surface water contents were being augmented continually by water, drawn up by evaporation and rising consolidation water.

4 DISCUSSION AND CONCLUSIONS

Current methods of calculating evaporation from soil surfaces are mostly based on the solar energy balance principle or on a form of Penman's equation in which the major input energy is the net incoming vertical component of solar energy and the major output is the latent heat of vaporization, LE, from which the evaporation is calculated. Current methods either ignore heating of the soil or assume that solar energy converted to soil heat detracts from LE.

Studies over the past decade have highlighted a number of difficulties with currently accepted methods of applying the solar energy balance calculation. These are:

1. The sun's rays strike the Earth's surface at an angle that varies throughout the day. Some of the energy is reflected and some heats the surface. However, the extent of the component that heats the surface is uncertain. Measurements of soil heat G and water heat WH show that the net vertical component is too small, but, because some reflection of energy does occur, the direct or maximum radiation must be too large (Figures 2 and 3).
2. In soils that are unsaturated or desiccated, the energy balance method over-estimates evaporation losses when compared with evaporation established by measured changes of water content (see Figures 4 and 5).
3. In sub-equatorial latitudes, the soil heat G and water heat WH may be as large, or larger than the measured net incoming vertical component of the solar energy, for much of the day. On the basis of equations (1c) and (1d), this suggests that in windless conditions, no evaporation will take place during this time (Figure 3). Measurements show that this is not so.
4. The present approach (equations (1c) and (1d)) leads to the conclusion that no evaporation occurs between sunset and sunrise because the incoming solar radiation is zero during this period. Common experience is that drying and therefore evaporation does occur at night, and this is shown by measurements reported in this paper (Figures 7 and 8).
5. Sections 3.5 and 3.6 illustrate the most difficult aspect of measuring evaporation from a soil surface—it is very difficult, in field measurements, to allow for the effects of water moving upwards under a suction or consolidation-induced flow gradient, or downwards under a gravity gradient.
6. The way ahead is by no means clear, but the difficulties associated with applying equation (1) and its derivatives should be noted, and if used, be used with caution. The substitution of R_n by G multiplied by a conversion efficiency η (eqn. 1d) is a route that warrants further examination.
7. Winter, et al. (1995), Rosenberry, et al. (2004, 2007) and Yao (2009) working in the closely related area of assessing evaporation from wetlands, reservoirs and lakes conclude that although application of the solar energy balance is, in theory, the best way to assess evaporation, it is difficult to apply in practice, mainly, in their case, because of time lags that occur between energy components entering storage and being transformed to evaporation. Similar time lags, such as the conversion of heat into evaporation after sunset, are evident even in the short term tests described in this paper.

REFERENCES

Benli, B., Bruggeman, A., Oweis, T. & Üstün, H. 2010. "Performance of Penman-Monteith FA056 in a Semi-arid Highland Environment." *Journal of Irrigation and Drainage Engineering*, ASCE, 136(11), 757–765.

Blight, G.E. 2005. Consequences of raising the height of a landfill in a water-deficient climate. *Waste Management*, 25, 1021–1036.

Blight, G.E. 2006a. Graded landfill requirements in South Africa: the climatic water balance classification. *Waste Management and Research,* 24(5), 482–490.

Blight, G.E. 2006b. Measuring evaporation from grassed surfaces and trees by energy balance. In: *Unsaturated Soils,* Miller, G.A., et al. (eds). Special Technical Publication No. 147, ASCE, Virginia, USA, 895–904.

Blight, G.E. 2008a. The repeatability of soil water balances at the same site from year to year. In: Unsaturated Soils: *Advances in Geo-Engineering.* Toll, D.G., et al. (eds), Taylor and Francis, London, UK, 889−894.

Blight, G.E. 2008b. Near-surface movement of water in unsaturated soil during evapotranspiration. In: Unsaturated Soils*: Advances* in *Geo-Engineering.* Toll, D.G., et al. (eds), Taylor and Francis, London, U.K. 895–900.

Blight, G.E. 2009a. Solar heating of the soil and evaporation from a soil surface. *Geotechnique*, 59(4), 355–363.

Blight, G.E. 2009b. Desiccation of soil by vegetation and potential interaction with buildings—a field study. *Jour. South African Institution of Civil Engineering,* 51(2), 20–29.

Blight, G.E. 2010. Geotechnical Engineering for Mine Waste Storage Facilities. CRC Press/Balkema, Leiden, Netherlands.

Blight, G.E. & Fourie, A.B. 2005. Experimental landfill caps for semi-arid and arid climates. *Waste Management and Research*, 23, 113–125.

Blight, G., Copeland, A., Jardine, P. & MacRobert, C. 2012. Measurements on freshly-deposited surfaces of two platinum tailings dams. *Paste* 2012, Jewell, R.J., et al. (eds). Australian Centre for Geomechanics, Perth, Australia, 11–24.

Calder, I.R. 1990. Evaporation in the uplands. Wiley, Chichester, UK.

de Bruin, H.A.R. & Keijman, 1979. The Priestley-Taylor evaporation model applied to a large, shallow lake in the Netherlands. *Journal of Applied Meteorology*, 18, 898–903.

Fenn, D.G., Hanley, K.J. & de Geare, T.Y. 1975. Use of the water balance method for predicting leachate generation from solid waste disposal sites. Report EPA/530/SW168. U.S. Environmental Protection Agency, Washington, USA.

Henken-Mellies, W.-U. & Schweizer, A. 2011. Long-term performance of landfill covers—results of lysimeter test fields in Bavaria (Germany). *Waste Management and Research*, 29(1), 59–68.

Monteith, J.L. 1980. The development and extension of Penman's evaporation formula. Applications of Soil Physics, Hillel D. (ed.). Academic Press, New York, USA, 265–275.

Oke, T.R. 1978. Boundary layer climates. Methuen, London, UK.

Penman, H.L. 1956. Estimating evaporation. Transactions, American Geophysical Union, 37, 43–50.

Penman, H.L. 1963. Vegetation and hydrology, Technical Communication No.53. Commonwealth Bureau of Soils, Commonwealth Agricultural Bureaux, Harpenden, UK.

Priestley, C.H.B. & Taylor, R.J. 1972. On the assessment of surface heat flux and evaporation using large-scale parameters. *Monthly Weather Review,* 100(2), 81–92.

Advances in Unsaturated Soils – Caicedo et al. (eds)
© 2013 Taylor & Francis Group, London, ISBN 978-0-415-62095-6

Interpretation of soil-water characteristic curves when volume change occurs as soil suction is changed

D.G. Fredlund
Golder Associates Ltd., Saskatoon, SK, Canada

S.L. Houston
School of Sustainable Engineering and the Built Environment, Arizona State University, Tempe, AZ, USA

ABSTRACT: The soil-water characteristic curve, SWCC, has become a valuable tool for the estimation of unsaturated soil property functions, USPF, in geotechnical engineering practice. At the same time, indiscriminate usage of the estimation techniques for unsaturated soils can lead to erroneous analytical results and poor engineering judgment. Soils that undergo significant volume changes as soil suction is changed constitute one situation where erroneous estimations can occur. In particular, it is the evaluation of the correct air-entry value for the soil that has a significant effect on the estimation of subsequent USPFs. This paper defines the characteristics of a high volume change material and then proceeds to describe how the SWCC laboratory results can be properly interpreted with the assistance of a shrinkage curve. Two laboratory data sets are presented and used to illustrate how the test data should be interpreted in the case of high volume change soils. There have also been developments in the design of SWCC laboratory equipment with the result that both overall volume change and water content change can be monitored when measuring SWCCs. As a result, all volume-mass properties can be calculated. One such apparatus is described along with a description of its benefits and limitations.

1 INTRODUCTION

The soil-water characteristic curve, SWCC, has become an important relationship to determine when applying unsaturated soil mechanics in engineering practice. The technologies related to the SWCC were originally developed in soil physics and agriculture-related disciplines. These technologies have slowly been embraced, with some modifications, in the application of unsaturated soil mechanics (Fredlund, 2002; Fredlund and Rahardjo, 1993).

Soil physics has primarily promoted the use of the SWCC within agriculture for the estimation of the water storage characteristics of soils near the ground surface. Unsaturated soil mechanics has primarily utilized the SWCC for the estimation of unsaturated soil property functions which are subsequently used in numerical modelling solutions of geotechnical engineering problems (Fredlund, 2010). It has long been recognized that there are independent drying and wetting branches for the SWCC, as well as an infinite number of scanning curves between the drying and wetting branches. However, the SWCC has often been treated in both agriculture and geotechnical engineering as though it were a single approximate relationship between the amount of water in a soil and soil suction. Within unsaturated soil mechanics, the drying (or desorption) SWCC branch has received the most attention. Disturbance of the soil samples has historically been of limited concern, or at least neglected, in both agriculture and geotechnical engineering, with disturbed and remolded soil samples often being used for laboratory testing.

Some of the concepts and measurement procedures for determining the relationship between the amount of water in a soil and soil suction (i.e., SWCC) are now receiving increased research interest as unsaturated soil mechanics is increasingly being used in geotechnical engineering applications. It was prudent and appropriate that consideration be given in geotechnical engineering to the wealth of knowledge that has accumulated within soil physics and agriculture. Along with the wealth of accumulated knowledge and experience, however, there are serious differences between the goals to be achieved in agriculture-related disciplines and the goals of geotechnical engineering. Unfortunately, many of these limitations have often been overlooked in the eagerness to make use of the SWCC. Unfortunately, the laboratory test procedures from soil physics and the application

of the SWCC theory in geotechnical engineering have not been fully researched prior to usage in geotechnical engineering. As a consequence, geotechnical engineers are now faced with the need to reconsider various aspects of the application of the SWCC. Some of the areas requiring further research for geotechnical engineering applications are highlighted in this paper.

2 THE PATH FORWARD

There are two approaches that could be taken with regard to further refinement in the application of the SWCC in unsaturated soil mechanics (Figure 1). First, it is possible that modified laboratory test procedures be developed and used for the measurement of the amount of water in the soil versus soil suction relationships in geotechnical engineering. It is also possible that new laboratory test equipment be designed to more realistically simulate field conditions. Second, it is possible that an additional, independent test be performed that would assist with the interpretation of a conventional gravimetric water content SWCC. An independent laboratory test that can be performed is a "shrinkage curve" test. The shrinkage curve test provides a fixed relationship between the gravimetric water content and the instantaneous void ratio of the soil. The authors would suggest that both of the above-mentioned approaches be given consideration. A review of the research literature shows that modified apparatuses for geotechnical applications have already become a trend for measuring the SWCC. Alternate testing procedures have also been proposed in the research literature. In particular, the need for a modification to the determination of an appropriate SWCC has arisen in situations where the soil changes volume as soil suction is changed.

The development of testing apparatuses that measure the SWCC under controlled suction and net normal stress, along with volume change measurements, is appealing for many geotechnical engineering problems (i.e., left branch in Figure 1). The approach that suggests adding a shrinkage test to assist in the interpretation of the SWCC (i.e., right branch in Figure 1), blends in well with the procedures that have already been used in engineering practice as well as agriculture-related disciplines. In other words, the existing laboratory test procedures associated with the SWCC would continue to be used; or available data sets used, however, greater care needs to be taken in the interpretation and application of the results in engineering practice. This approach may be particularly appealing when net normal stress is relatively low in the field application.

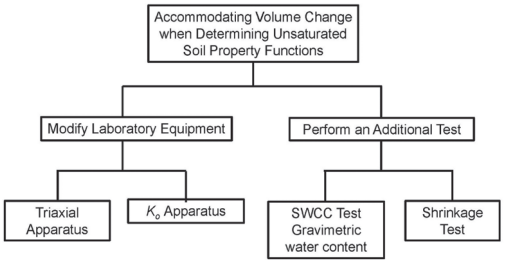

Figure 1. Approaches that can be taken to accommodate volume changes associated with soil suction changes.

This paper presents information on both of the above-suggested options for accommodating volume change that occurs as a result of soil suction changes. The paper also describes the procedures related to the determination of appropriate SWCCs for geotechnical engineering practice. The scope of the paper embraces consideration of sand, silt and clay textured soils and the differences involved in the interpretation of the laboratory results. Differences in interpretation primarily depend upon the amount of volume change experienced during the application of soil suction at a given net normal stress. Another objective is to illustrate the importance of the shrinkage curve in interpreting the SWCC laboratory test results. Laboratory test results are presented for highly plastic soils that are initially prepared in a slurry condition. These materials undergo significant volume change as soil suction is increased. Data is obtained using modified K_o equipment to determine the SWCC curve, with volume change, on a compacted expansive soil.

3 EXAMPLES OF VOLUME CHANGE AS SOIL SUCTION IS CHANGED

The conventional application of the SWCC for the estimation of unsaturated soil property functions commences with the assumption that the soil does not significantly change volume as soil suction is increased. This assumption may be reasonable for low compressibility sands, silts and dense coarse-grained soils. However, there are other situations where the geotechnical engineer must determine unsaturated soil property functions when the soil undergoes considerable volume change with changes in soil suction. Such applications include wetting and drying of expansive clays, wetting of collapsible soils, and drying of slurry materials.

A common situation where extreme volume change occurs in the soil as soil suction is increased, involves the drying of initially wet or slurry materials. Sludge material and slurry material (e.g., Mature Fine Tailings, MFT, from the Oil

Sands operation), are deposited at water contents well above the liquid limit of the material (e.g., w = 100%). The material is deposited in ponds and allowed to dry in order to increase its shear strength. The geotechnical engineer is called upon to undertake numerical modelling simulations of the drying process. Volume changes in excess of 100% are common, and failure to take volume change into consideration yields erroneous results during the drying simulation.

Almost any situation where a soil starts under very wet conditions and is subjected to drying will result in significant volume change. The material may be initially saturated and may remain near saturation, as soil suction increases during the drying process. Estimation procedures that have historically been proposed for the calculation of unsaturated soil property functions assume that a decrease in water content corresponds to a decrease in the degree of saturation of the soil. This may not always be the case and consequently the estimation procedures will give erroneous results when either gravimetric water content or volumetric water content SWCCs are used to calculate unsaturated soil properties such as the permeability functions.

Expansive soils problems are often associated with the soil taking on water as a result of infiltration. This is an adsorption process that involves the wetting SWCC. The effect of hysteresis needs to be taken into consideration as well as the effect of volume changes that occur as the soil dries or goes towards saturation.

Collapsible soils follow a different drying stress path than wetting stress path. The collapsible soil may initially be in a relatively dry state with substantial soil suction. As the soil imbibes water the volume of the soil decreases (or collapses). This has been a difficult stress path to simulate through numerical modelling. Volume change as soil suction is decreased has an effect on the determination of suitable unsaturated soil property functions.

This paper mainly focuses on the estimation of suitable SWCCs for soils that have high initial water content. At the same time it is recognized that there may be other stress paths that might need to be simulated in geotechnical engineering practice. This paper also discusses the benefits that can be accrued through use of modified pressure plate apparatuses for the measurement of the SWCC.

4 DESCRIPTION OF SWCC TEST PROCEDURES COMMONLY USED IN SOIL PHYSICS

Historically, soil specimens have been initially saturated, placed on a pressure plate apparatus under very light confining stress and subjected to increasing matric suction values while equilibrium water contents were measured. The equilibrium water content (for each applied matric suction), was generally established in one to three days depending upon the soil type. Applied air pressures were applied to the soil specimen(s) and the matric suction was established through use of the axis-translation technique. Pressure plate apparatuses were developed that either tested one or multiple soil specimens simultaneously.

Matric suction values were increased on a logarithm scale (i.e., doubling the applied air pressure), until the air-entry value of the ceramic pressure plate was reached. The ceramic pressure plates generally had air-entry values ranging from 100 kPa to 1,500 kPa. The high range of soil suctions (i.e., beyond 1,500 kPa), were generally applied using vapour pressure equalization of small soil samples placed above saturated salt solutions in a vacuum desiccator.

Changes in the amount of water in the soil were either determined through measurement of changes in the overall mass of the soil specimens or the change in the volume of water expelled from the soil under each applied matric suction. In either case, the laboratory results were generally presented as a graph of volumetric water content on the ordinate versus the logarithm of soil suction. The assumption was made that the initial soil specimen was initially saturated. A second assumption was also made in presenting the laboratory results; namely, that the overall volume of the soil specimens did not change as the applied soil suction were increased. This assumption allowed measurements of changes in the mass of water in the soil to be used to back-calculate volumetric water contents for all applied soil suction values.

The above-mentioned testing procedure has served the agriculture-related disciplines quite well where the primary objective was to quantify the water storage in the soil under various applied suction conditions. It should be noted that while the SWCC used in agriculture is usually plotted as a graph of volumetric water content versus soil suction, the plot is only rigorously correct provided there is no volume change as soil suction is increased. All changes in the mass or volume of water removed as soil suction is changed are referenced back to the original volume of the soil specimen. It should be noted that volumetric water content is rigorously defined as the volume of water in the soil referenced to the instantaneous overall volume. Consequently, volumetric water content is correctly defined from gravimetric water content change alone only when no overall volume change occurs.

5 DESCRIPTION OF SWCC TEST PROCEDURES COMMONLY USED IN GEOTECHNICAL ENGINEERING

The purpose for which the SWCC laboratory results are used in geotechnical engineering is quite different from that of the agriculture disciplines and as a result, questions arise as to whether it is necessary to change the SWCC test procedure, the interpretation procedure or both. This paper shows that application of the SWCC in geotechnical engineering is somewhat different from applications in agriculture, primarily because soil volume change in response to wetting and loading for many geotechnical engineering applications can be substantial.

Test procedures that had been used in agriculture for several decades began to be used in geotechnical engineering subsequent to 1960 (Fredlund, 1964). The need to measure the SWCC became apparent when it was realized that changes in the suction of a soil produced an independent effect on soil behavior from changes in total stress. Engineering problems associated with expansive soils provided the initial impetus for understanding swelling soil behavior in terms of changes in soil suction. In most cases, the expansive soils had substantial clay content and underwent considerable volume change during the swelling process associated with wetting. In addition, subsequent applications of matric suction resulted in a decrease in the volume of the soil specimens. There are other applications of unsaturated soil mechanics in geotechnical engineering that involve soil volume change due to change in soil suction. Examples involve the drying of initially slurry materials and the wetting of collapsible soils. For drying of initially slurried soils there can be extremely large volume changes associated with the application of soil suction.

The primary application of SWCCs in geotechnical engineering has been for the estimation of unsaturated soil properties such as permeability function (i.e., hydraulic conductivity versus soil suction) (e.g., Fredlund et al., 1994; van Genutchen, 1980), and the shear strength function, (i.e., shear strength versus soil suction) (e.g., Vanapalli et al., 1996; Fredlund et al., 1996). The estimation of realistic hydraulic conductivity functions depends on the separation of volume changes that might occur while the soil remains saturated from volume changes that occur as the soil desaturates.

Conventional testing procedures adopted within soil physics have not made a clear distinction between these two volume change mechanisms. Direct acceptance and adoption of soil physics SWCC testing procedures can result in serious deficiencies when testing materials that undergo volume change as soil suction is increased. Stated another way, it is not sufficient to measure changes in the mass or volume of water removed from the soil between various applied soil suctions. Rather, it is necessary to quantify the amount of volume change that occurs and to separate the volume changes that occur while the soil remains saturated from the volume changes (and water content changes) that occur as the soil desaturates. The estimation procedures for unsaturated soil property functions is different when the soil is undergoing volume change from the situation where there is no volume change as soil suction is changed.

The differences in physical processes associated with the two types of volume change give rise to the need to be able to measure both changes in the volume of water mass as well as actual (or instantaneous) volume changes of the soil specimen. Two approaches to addressing this need for volume change measurements are considered in this paper. The first approach considers modifying the laboratory SWCC apparatuses such that the volume of the soil specimens is measured during the test. Devices that have been developed to meet this need are discussed later in this paper. The second approach suggests using an independent test to measure the relationship between gravimetric water content and void ratio. The required laboratory test is referred to as a shrinkage test and details related to this procedure are subsequently outlined in this paper.

6 USE OF SIGMOIDAL EQUATIONS FOR SWCCS

There are several sigmoidal type equations that have been proposed to mathematically describe the water content versus soil suction relationship (e.g., van Genuchten, 1980; Fredlund and Xing, 1994). The sigmoidal equations are S-shaped and have the appearance of being able to fit SWCC data regardless of the measure that is used to represent the amount of water in the soil (e.g., gravimetric water content, volumetric water content, or degree of saturation). The sigmoidal equations have a limitation in the extremely low suction range and the extremely high suction range as shown in Figure 2. In spite of the shortcomings of the sigmoidal equations their usage has become prevalent in unsaturated soil mechanics.

The Fredlund and Xing (1994) SWCC equation will be used to illustrate the character and usage of a sigmoidal equation for various designations of water content. The Fredlund and Xing (1994) equation makes use of a correction factor that allows all SWCCs to go to zero water content as soil suction goes to 1,000,000 kPa. Laboratory measured SWCC data can be plotted as a relationship between gravimetric water content and soil suction. The Fredlund and Xing (1994) equation (Equation 1) can then be used to best-fit the SWCC.

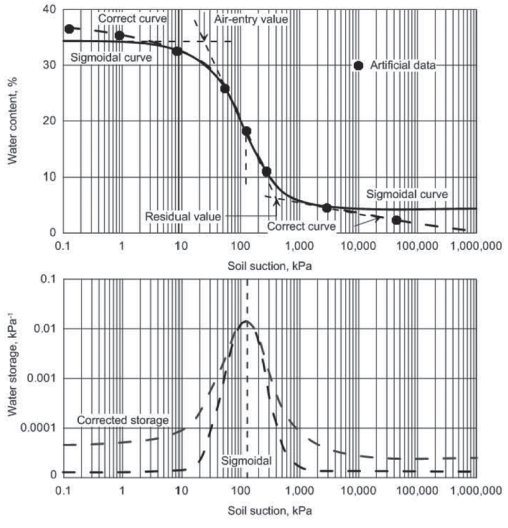

Figure 2. Limitations in the fitting of a sigmoidal equation to SWCC data.

$$w(\psi) = w_s \left[1 - \frac{\ln\left(1 + \frac{\psi}{h_r}\right)}{\ln\left(1 + \frac{10^6}{h_r}\right)} \right] \times \left[\frac{1}{\left[\ln\left[\exp(1) + \left(\frac{\psi}{a_f} \right)^{n_f} \right] \right]^{m_f}} \right] \quad (1)$$

where: $w(\psi)$ = gravimetric water content at any specified suction, ψ; w_s = saturated gravimetric water content; h_r = residual soil suction; a_f, n_f, and m_f = the fitting parameters for the Fredlund and Xing (1994) SWCC equation. Equation 1 is written for the gravimetric water content designation; however, the equation could also be best-fit to any of the designations of water content (e.g., volumetric water content or degree of saturation) versus soil suction. The gravimetric water content SWCC will be used in conjunction with the shrinkage curve to interpret the parameters required for the estimation of unsaturated soil property functions.

It is possible to compute and best-fit the degree of saturation versus soil suction as well as any other designation for the amount of water in the soil by combining Equation 1 with the volume-mass relations for an unsaturated soil. The shrinkage curve for a soil provides information on changes in overall volume as soil suction is changed.

The volumetric water content versus soil suction SWCC must be differentiated with respect to soil suction to obtain the water storage coefficient for the soil. The volumetric water content must be related to the instantaneous overall volume of the soil mass in order to obtain the correct value for numerical modelling purposes. Volume change of the overall soil specimen can be taken into consideration if the relationship between gravimetric water content, w, and void ratio, e, is known. This relationship can be referred to as the "shrinkage curve" when the net normal stress is zero.

7 NEED FOR A SHRINKAGE CURVE

A graphical representation of void ratio versus gravimetric water content can be used to illustrate a variety of volume-mass pathways that might be followed for a particular geotechnical engineering problem involving unsaturated soils. Figure 3 shows typical volume-mass paths for: (a) an initially slurried, high plasticity soil that is dried from a high water content; (b) a swelling soil that is allowed to wet from an initially dry condition; (c) a silt or sand soil that does not undergo volume change as the soil is either dried or wetted; and (d) a collapsible soil that is wetted from a relatively dry initial state. The scope of this paper is limited to consideration of the drying of soils that are initially in a slurry state. Other volume-mass paths should be the focus of further research since the overall volume change of a soil as suction is changed, influences the estimation of unsaturated soil property functions.

The shrinkage limit of a soil has been one of the classification properties in soil mechanics (ASTM D427). Mercury immersion was originally used for the measurement of the volume of a soil specimen. The technique is no longer considered acceptable in most countries. The shrinkage limit is defined as the water content corresponding to a saturated specimen at the void ratio achieved (minimum volume) upon drying to zero water content. It is the entire shrinkage curve, the plot of total volume (or void ratio) versus gravimetric water content, from an initially saturated soil condition to completely oven-dry conditions that is significant for the interpretation of SWCC data.

As saturated clay soil dries, a point is reached where the soil starts to desaturate. This point is called the air-entry value and is generally near the plastic limit of the soil. Upon further drying, another point is reached where the soil dries without significant further change in overall volume. The corresponding gravimetric water content appears to be close to that corresponding to the residual soil suction.

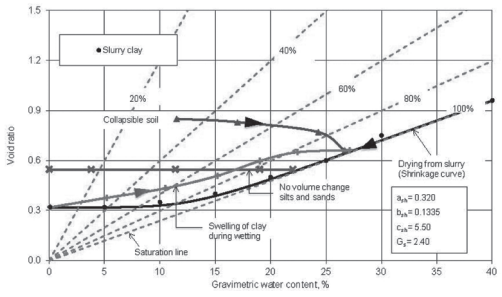

Figure 3. Volume-mass pathways for a variety of possible geotechnical engineering situations.

Figure 4. Digital micrometer used for the measurement of the diameter and thickness of shrinkage specimens.

The shrinkage curve can be experimentally measured from initial high water content conditions to completely dry conditions. A digital micrometer can be used for the measurement of the volume at various stages of drying as shown in Figure 4. Brass rings can be machined to contain the soil specimens (i.e., the rings have no bottom). The rings with the soil can be placed onto wax paper and can be dried through evaporation to the atmosphere. The dimensions of the soil specimens are appropriately selected such that cracking of the soil is unlikely to occur during the drying process. The initial dimensions selected for the shrinkage curve specimens used in this study were a diameter of 3.7 cm and a thickness of 1.2 cm.

The mass and volume of each soil specimen can be measured once or twice per day. Four to six measurements of the diameter and thickness of the specimen were made at differing locations on the specimens. It has been observed that as the specimen diameter began to decrease, with the specimen pulling away from the brass ring, the rate of evaporation increased significantly (i.e., about twice as fast).

The increase in the evaporation rate is related to the increased surface area from which evaporation occurs. Consequently, it is recommended that the measurements of mass and volume be increased to once every two to three hours once the material shows signs of pulling away from the sides of the ring.

The "shrinkage curve" can be best-fit using the hyperbolic curve proposed by Fredlund et al., (1996, 2002). The equation has parameters with physical meaning and is of the following form:

$$e(w) = a_{sh}\left[\frac{w^{c_{sh}}}{b_{sh}^{c_{sh}}} + 1\right]^{\left(\frac{1}{c_{sh}}\right)} \qquad (2)$$

where: a_{sh} = the minimum void ratio (e_{min}), b_{sh} = slope of the line of tangency, (e.g., = e / w when drying from saturated conditions), c_{sh} = curvature of the shrinkage curve, and w = gravimetric water content. The ratio, $\frac{a_{sh}}{b_{sh}} = \frac{G_s}{S_r}$ is a constant for a specific soil; G_s is the specific gravity and S is the degree of saturation.

Once the minimum void ratio of the soil is known, it is possible to estimate the remaining parameters required for the designation of the shrinkage curve. The minimum void ratio the soil can attain is defined by the variable, a_{sh}. The b_{sh} parameter provides the remaining shape of the shrinkage curve. The curvature of the shrinkage curve around the point of desaturation is controlled by the c_{sh} parameter.

8 DIFFERENT DESIGNATIONS FOR THE AMOUNT OF WATER IN THE SOIL

There are three primary ways to designate the amount of water in the soil; namely, gravimetric water content, volumetric water content and degree of saturation. Each designation has a role to play in understanding the physical behaviour of unsaturated soils.

8.1 *Gravimetric water content*

The measurement of water content in the laboratory is generally first measured in terms of gravimetric water content, w, because the mass of water is the easiest variable to measure. Other designations are then computed based on the volume-mass relations. The gravimetric water content SWCC was presented in Equation 1.

8.2 *Volumetric water content (instantaneous volume)*

Volumetric water content can be written as a function of the instantaneous overall volume of the soil

specimen, $(1 + e)$, and gravimetric water content, w. Since gravimetric water content can be expressed as a function of soil suction, it is likewise possible to write volumetric water content as a function of soil suction.

$$\theta(w) = \frac{w(\psi)G_s}{1 + e(w)} \tag{3}$$

The equation for the void ratio can be substituted into Equation 3 to yield the volumetric water content equation in terms of gravimetric water content along with several soil parameters.

$$\theta(w) = \frac{w(\psi)G_s}{1 + a_{sh}\left[\frac{w(\psi)}{b_{sh}^{\,c_{sh}}} + 1\right]^{1/c_{sh}}} \tag{4}$$

8.3 *Degree of saturation*

The degree of saturation of the soil can be written as a function of gravimetric water content (as a function of suction) and void ratio (as a function of gravimetric water content).

$$S(w) = \frac{w(\psi)G_s}{e(w)} \tag{5}$$

The degree of saturation can be further written as a function of gravimetric water content and the equation for the shrinkage curve, both which are functions of soil suction.

$$S(\psi) = \frac{w(\psi)G_s}{a_{sh}\left[\frac{w(\psi)}{b_{sh}^{\,c_{sh}}} + 1\right]^{1/c_{sh}}} \tag{6}$$

The degree of saturation SWCC can also be written as a function of soil suction and the fitting parameters for the gravimetric water content SWCC and the shrinkage curve.

$$S(\psi) = \frac{w_s G_s C_r(\psi_r)}{\left[\ln\left[\exp(1) + (\psi/a_f)^{n_f}\right]^{m_f} \times a_{sh}\left[\frac{w_s G_s C_r(\psi_r) b_{sh}^{\,c_{sh}}}{\ln\left[\exp(1) + (\psi/a_f)^{n_f}\right]^{m_f}}\right] + 1\right]^{1/c_{sh}}} \tag{7}$$

8.4 *Volumetric water content (initial volume)*

It is possible to write the volumetric water content referenced to the initial volume of the soil; however, it should be noted that this designation has little or no value in unsaturated soil mechanics. Only under conditions of no volume change during suction change does the equation become equal to the instantaneous volumetric water content SWCC.

$$\theta(w) = \frac{w(\psi)G_s}{1 + e_o} \tag{8}$$

8.5 *Void ratio*

The void ratio versus soil suction is of value in some situations. One such situation occurs when attempting to describe volume changes while the soil remains saturated under an applied suction. The void ratio can be written as a function of gravimetric water content which is a function of soil suction (i.e., shrinkage curve designated by Equation 2).

8.6 *Experimental and parametric study program on the effect of volume changes on the interpretation of the SWCC*

The effect of volume change on the interpretation of SWCCs was studied using the results from two experimental studies. For both soils, the laboratory SWCCs and shrinkage curve measured on initially slurried soils. The two materials were: (1) Oil Sands Tailings referred to as MFT (Mature Fine Tailings), and (2) Regina clay. The laboratory test results are first presented followed by a parametric study that focuses on the significance of overall volume change as soil suction is increased.

A parametric study was also undertaken for each of the two materials. The parametric study involved changing two of the fitting parameters in the gravimetric water content SWCC. For the Oil Sands Tailings, the first break in curvature along the gravimetric water content SWCC, (referred to as *w Break*), was maintained constant. For the Regina clay soil, the air-entry value, AEV, determined from the degree of saturation SWCC was kept constant. In each case, an empirical construction procedure involving the intersection of two straight lines on a semi-log plot was used to determine a single number for the break in curvature (Vanapalli et al., 1999).

8.7 *Oil sands tailings*

The laboratory program on the Oil Sands tailings involved the measurement of the gravimetric water

content SWCC and the shrinkage curve. The Oil Sands Tailings were prepared with sand to fines ratio, SFR, of 0.1. The liquid limit was 55%, plastic limit 22%, and specific gravity, G_s, was 2.40. Approximately 60% of the material classifies as clay size particles.

The analysis of the test results assumed that the initial starting (saturated) gravimetric water content was increased while the remaining curve-fitting parameters were kept constant. In other words, the first break in curvature along the gravimetric water content SWCC, (*w Break*), was kept constant. Changes in the air-entry values from the degree of saturation SWCC, (i.e., AEV or air-entry value) were then determined.

If the soil did not undergo any volume change, then the "*w Break*" and the AEV would be equal, or the ratio of AEV to *w Break* would be equal to 1.0. Consequently, the ratio of AEV to *w Break* can be used as a measure of the effect of volume change on the interpretation of the correct air-entry value for the soil.

8.8 *Regina clay*

The Regina clay had a liquid limit of 75%, a plastic limit of 25% and contained 50% clay size particles. The material was prepared as slurry and then subjected to various consolidation pressures under one-dimensional loading. After the applied load was removed, the soil specimens were subjected to various applied matric suction values. High suction values were applied through equalization in a constant relative humidity environment. The parametric study then assumed that the air-entry value determined from the degree of saturation SWCC remained at a constant value. (This was confirmed by the experimental results). The "*w Break*" on the gravimetric water content SWCCs were then compared to the air-entry value for the soil. The ratio of AEV to *w Break* was used as a measure of the effect of volume change on the interpretation of the correct air-entry value for the soil.

8.9 *Presentation of the laboratory measurements on oil sands tailings*

Shrinkage curves and soil-water characteristic curves were measured on Oil Sands tailings samples prepared with 10% sand added (i.e., SFR = 0.1). The slurry material has a gravimetric water content of about 100%. The shrinkage curve results are presented in Figure 5. The volume of the Oil Sands tailings decreases as water is removed through evaporation. The material begins to desaturate near the plastic limit.

Figure 6 shows the gravimetric water content, *w*, plotted versus soil suction for the Oil Sands

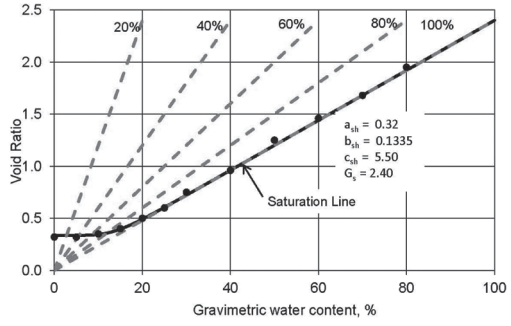

Figure 5. Average laboratory shrinkage curves for the Oil Sands Tailings samples tested (SFR = 0.1).

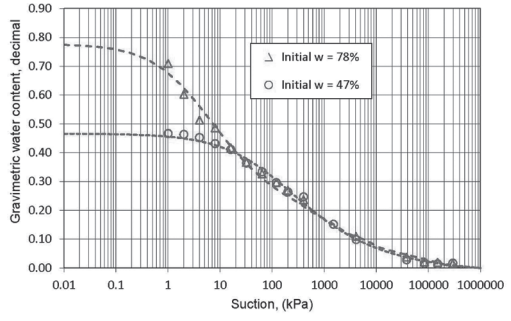

Figure 6. Gravimetric water content SWCC's measured on the Oil Sands tailings (SFR = 0.1).

tailings. One specimen was tested with the initial gravimetric water content near 78% and a second specimen was dried to a water content of 47% and then tested.

The initially high water content specimen showed a break in the curvature in the region around 1 kPa. The lower water content specimen (i.e., 47%) showed a break in curvature around 10 kPa. However, the curvature is not distinct and does not represent the true air-entry value of the material. It is necessary to use the shrinkage curve results in order to properly interpret the SWCC results.

A best-fit shrinkage curve equation can be combined with the equation for the Fredlund and Xing (1994) equation for the SWCC. The resulting plot of degree of saturation, *S*, versus soil suction is shown in Figure 7. The results show that there is a distinct air-entry value for the Oil Sands tailings at about 1,000 kPa. The true air-entry value is the same for the material with initial water contents of 78% and 47%. The results would indicate that it is more correct to use the degree of saturation SWCCs for the estimation of the unsaturated hydraulic conductivity function once the material

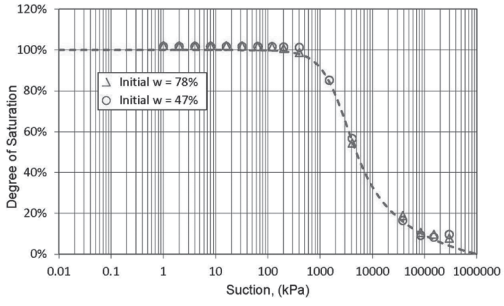

Figure 7. SWCC's plotted as the degree as saturation versus suction for the Oil Sands tailings (SFR = 0.1).

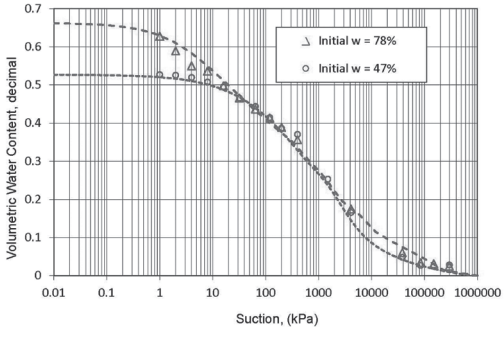

Figure 8. Volumetric water content versus suction for the Oil Sands tailings (SFR = 0.1).

began to desaturate. The degree of saturation plot also indicates that residual condition can be identified at a suction of about 15,000 kPa and a residual degree of saturation of about 20%.

Figure 8 shows the volumetric water content versus soil suction plots for the Oil Sands tailings. These curves appear to be similar in shape to the gravimetric water content plots. The volumetric water content curves are required when quantifying the water storage function for the material.

The basic volume-mass relationship, (i.e., $Se = wG_s$) also makes it possible to plot void ratio, e, versus soil suction as shown in Figure 9. The curves show that there is essentially no volume change at soil suctions higher than the residual suctions.

9 PARAMETRIC STUDY AND INTERPRETATION OF THE OIL SANDS TAILINGS RESULTS

A parametric analysis was performed to quantify the effect of various amounts of volume change on the determination of the correct air-entry value.

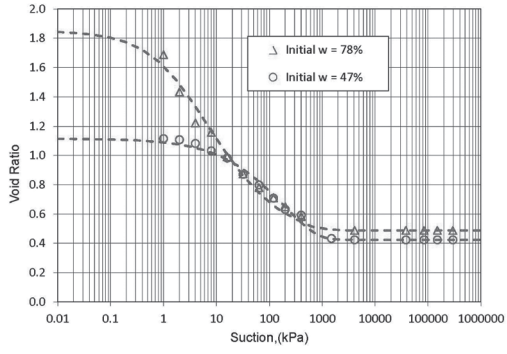

Figure 9. Void ratio versus suction plot for the Oil Sands tailings (SFR = 0.1).

The volume change is assumed to occur as a result of increases in soil suction as the material dries. The degree of saturation SWCC was assumed to remain the same for all soils tested. The initial condition of each soil tested was saturated. The best-fit parameters for the gravimetric water content SWCC were determined for the material tested at 78% initial water content and maintained constant for all other initial saturated water content conditions.

The initial saturated water content of the specimen controlled the amount of volume change that would occur as the soil specimen was subjected to increased suction. The amount of volume change that occurred between the initial low suction value and the residual suction conditions was computed as the change in void ratio, Δe, divided by $(1 + e_o)$ where e_o is the residual void ratio. All void ratio values were determined from the measured shrinkage curve.

Figure 10 shows the difference between the break in curvature on the gravimetric water content SWCC and the true AEV obtained from the degree of saturation SWCC plotted versus percent volume change experienced by the soil. A starting water content equal to the residual water content meant that no volume change occurred and the ratio of the break in the gravimetric water content SWCC was equal to the break in the true AEV observed on the degree of saturation SWCC.

When the starting water content was such that 10% volume change took place during the gravimetric water content SWCC test, the break in the degree of saturation curve was 6 times larger than the break in curvature from the gravimetric water content SWCC. Likewise, when the starting water content was such that 20% volume change took place during the gravimetric water content SWCC test, the break in the degree of saturation curve was 16 times larger than the break in curvature from the gravimetric water content SWCC. Forty percent volume change was also quite feasible and in this case, the break in the degree of saturation

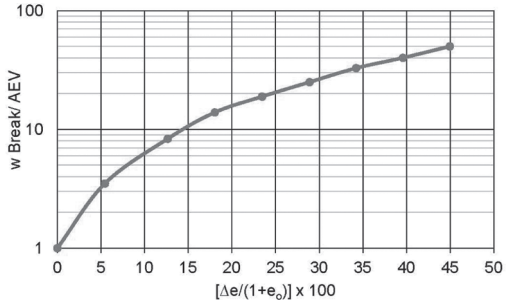

Figure 10. Ratio of the break in the gravimetric water content plot to the true Air-Entry Value for the Oil Sands tailings.

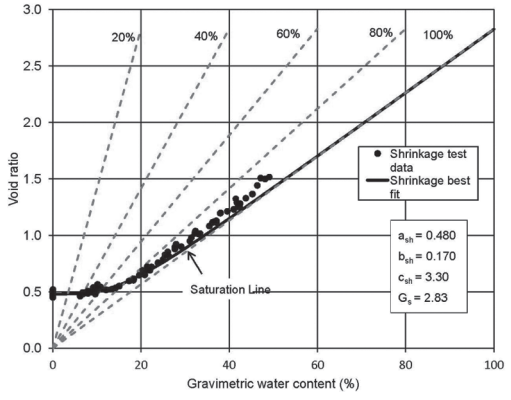

Figure 11. Shrinkage curve for several samples of Regina clay.

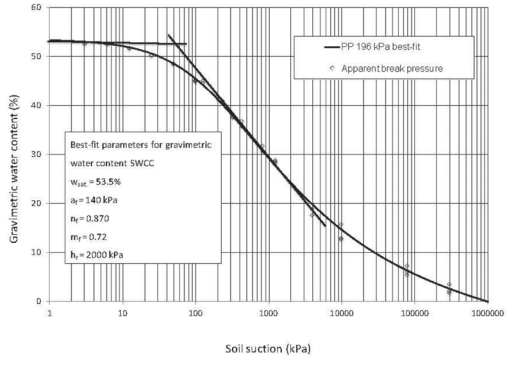

Figure 12. Gravimetric water content versus soil suction for Regina clay preconsolidated to 196 kPa.

curve was 40 times larger than the break in curvature from the gravimetric water content SWCC. Needless to say, volume changes during suction increases in clayey soils can significantly change the interpretation of SWCC test results.

There are a number of estimation procedures that make use of the SWCC for calculating the permeability function of the soil. Each of these estimation procedures calculate the possible decrease in hydraulic conductivity as the material desaturates. Consequently, it is necessary to separate the changes in hydraulic conductivity that are related to void ratio change (under saturated conditions) from changes in degree of saturation.

10 PRESENTATION OF THE LABORATORY MEASUREMENTS ON REGINA CLAY

Shrinkage curves and soil-water characteristic curves were measured on Regina clay. Slurry Regina clay was prepared at a gravimetric water content slightly above its liquid limit. The shrinkage curve results are presented in Figure 11. The void ratio of Regina clay decreases as water evaporates from the soil surface. The clay begins to desaturate near its plastic limit. The best-fit parameters for the shrinkage curve are $a_{sh} = 0.48$, $b_{sh} = 0.17$, and $c_{sh} = 3.30$. The specific gravity of the soil was 2.73.

Figure 12 shows the gravimetric water content, w, plotted versus soil suction for Regina clay was preloaded at 196 kPa. Its initial water content was 53.5%. The initially high water content specimen showed that a gradual break or change in curvature occurred around 50 kPa. The curvature is not distinct and does not represent the true air-entry value of the material. The gravimetric water content SWCC was best-fit with the Fredlund and Xing (1994) equation and yielded the following parameters; that is, $a_f = 140$ kPa, $n_f = 0.87$, and $m_f = 0.72$. Residual suction was estimated to be around 200,000 kPa. It is necessary to use the shrinkage curve to calculate other volume-mass soil properties and properly interpret the SWCC results for the true AEV.

The best-fit shrinkage curve equation can be combined with the equation for the Fredlund and Xing (1994) equation for the SWCC. The resulting plot of degree of saturation, S, versus soil suction is shown in Figure 13. The results show that there is a distinct air-entry value for Regina clay is about 2,500 kPa. The true air-entry value was also found to be the same for all Regina clay samples preconsolidated at differing pressure values. It is more correct to use the degree of saturation SWCCs for the estimation of the AEV of the soil and subsequently the unsaturated hydraulic conductivity function. The degree of saturation also indicates that residual condition can be more clearly identified as being at a suction of about

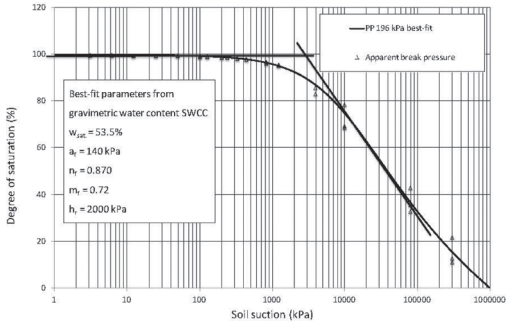

Figure 13. Degree of saturation versus soil suction for Regina clay preconsolidated to 196 kPa.

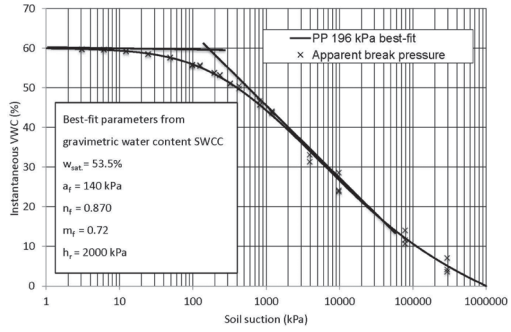

Figure 14. Instantaneous volumetric water content, VWC, versus soil suction for Regina clay preconsolidated to 196 kPa.

200,000 kPa and a residual degree of saturation of about 20 percent.

Figure 14 presents a plot of instantaneous volumetric water content, VWC, versus soil suction for the Regina clay preconsolidated at 196 kPa. The break in curvature is similar to that observed when using the gravimetric water content. While the VWC plot does not reveal the true AEV, it is the volumetric water content plot that must be differentiated with respect to soil suction in order to compute the water storage under any soil suction.

Figure 15 shows still another plot of water content versus soil suction conditions. In this case, gravimetric water content is non-dimensionalized by dividing by the saturated gravimetric water content. The break in curvature occurs around a value of about 46 kPa; a number similar to that observed on the gravimetric water content plot. The water content conditions are plotted in a dimensionless manner but this does not assist with the interpretation of meaningful characteristics on the SWCC.

Figure 16 shows a plot of void ratio versus soil suction conditions. There is a break in the curvature of the graph around 45 kPa; however, it should be noted that the true AEV determined from the degree of saturation graph showed that the value was about 2,500 kPa. This means that the soil did not start to desaturate until the void ratio was about 0.7 (or the water content was about 25% which is near the plastic limit of the soil). The minimum void ratio achieved upon complete shrinkage was 0.48.

Several other SWCC tests were performed on the Regina clay; each test starting with soil that had been preconsolidated from slurry to differing applied pressures. Figure 17 shows the gravimetric water content versus soil suction plot for a soil preconsolidated to 6.125 kPa. The Fredlund and Xing (1994) fitting parameters are a_f = 18.0 kPa,

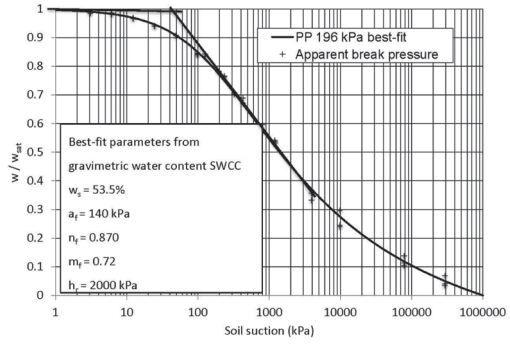

Figure 15. w/w_{sat} versus soil suction for Regina clay preconsolidated to 196 kPa.

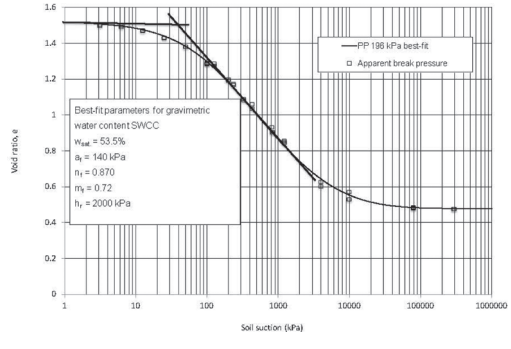

Figure 16. Void ratio versus soil suction for Regina clay preconsolidated to 196 kPa.

n_f = 0.88, m_f = 0.76 and h_r = 800 kPa. The degree of saturation SWCC is the same as shown in Figure 13.

Figure 18 shows the gravimetric water content versus soil suction plot for a soil preconsolidated to 12.25 kPa. The Fredlund and Xing (1994) fitting

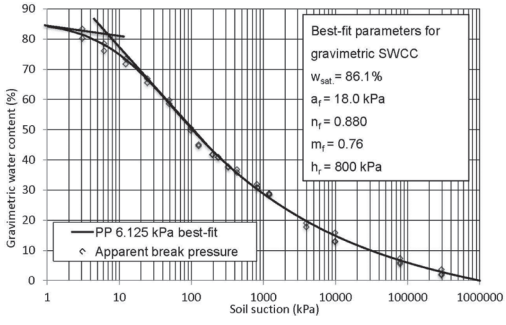

Figure 17. Gravimetric water content versus soil suction for Regina clay preconsolidated to 6.125 kPa.

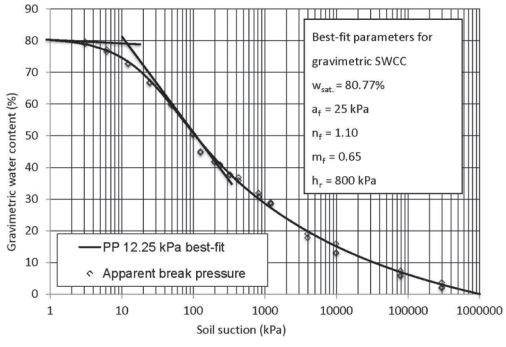

Figure 18. Gravimetric water content versus soil suction for Regina clay preconsolidated to 12.25 kPa.

parameters are a_f = 25.0 kPa, n_f = 1.10, m_f = 0.65 and h_r = 800 kPa. The best-fit parameters can readily describe the shape of the entire gravimetric water content SWCC. However, an understanding of the physical behavior of the Regina clay must be carefully gleaned through interpretation of several SWCCs using different water content representations when there is volume change as soil suction is increased.

Figure 19 shows the gravimetric water content versus soil suction plot for a soil preconsolidated to 24.5 kPa. The Fredlund and Xing (1994) fitting parameters are a_f = 40.0 kPa, n_f = 1.30, m_f = 0.58 and h_r = 1000 kPa. Figure 20 shows the gravimetric water content versus soil suction plot for a soil preconsolidated to 49.0 kPa. The Fredlund and Xing (1994) fitting parameters are a_f = 90.0 kPa, n_f = 1.10, m_f = 0.70 and h_r = 2000 kPa. Figure 21 shows the gravimetric water content versus soil suction plot for Regina clay preconsolidated to the highest pressure of 392 kPa. The Fredlund and Xing (1994) fitting parameters are a_f = 120.0 kPa, n_f = 0.84, m_f = 0.70 and h_r = 2000 kPa.

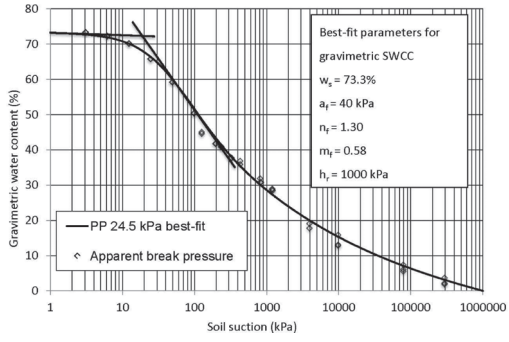

Figure 19. Gravimetric water content versus soil suction for Regina clay preconsolidated to 24.5 kPa.

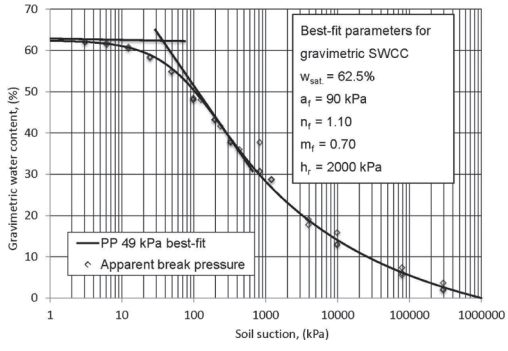

Figure 20. Gravimetric water content versus soil suction for Regina clay preconsolidated to 49 kPa.

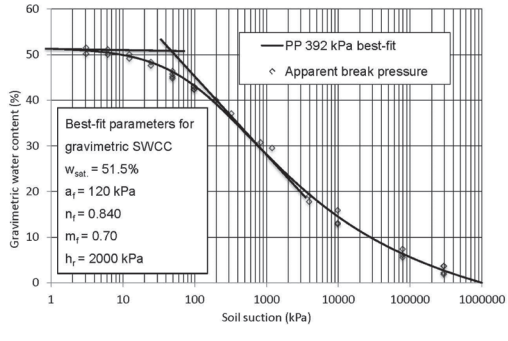

Figure 21. Gravimetric water content versus soil suction for Regina clay preconsolidated to 392 kPa.

The measured SWCCs for Regina clay show that the measurement of the gravimetric water content SWCC and the shrinkage curve for a soil are all that is required to obtain an approximation of the volume-mass versus soil suction relationships when the applied net normal stress is zero. The procedure that should be used for the interpretation of the laboratory data has also been described.

11 INTERPRETATION OF THE RESULTS ON REGINA CLAY

A similar procedure to that used for interpreting the Oil Sands tailings can be used to explain the significance of the measurements on Regina clay (See Figure 22). However, this time the difference between the break in the gravimetric water content SWCC and the true AEV will be expressed in an inverse manner (i.e., AEV/(Break in curvature on w SWCC)). The volume change of the soil is once again expressed as the change in void ratio, Δe, divided by $(1 + e)$ and all void ratio values are determined from the shrinkage curve.

The horizontal axis of Figure 22 shows that the Regina clay soil specimens changed in volume by 65% to 150% as soil suction was increased to residual suction conditions. At 70% volume change, the true AEV is 60 times larger than the break in curvature indicated by the gravimetric water content SWCC. Also at 120% volume change, the true AEV is 129 times larger than the break in curvature indicated by the gravimetric water content SWCC. The laboratory test results clearly indicate the significant influence that volume change as soil suction increases has on the interpretation of the data.

Further research should be undertaken to verify that the unsaturated soil property functions can indeed be estimated by using the interpretations suggested in this paper.

12 EQUIPMENT MODIFICATIONS TO MEASURE OVERALL VOLUME CHANGE

Equipment in common use for measuring this soil-water characteristic (Tempe cell, pressure membrane, pressure plate), often lacks some features that are important to the study of unsaturated soil behavior for geotechnical applications. These features involve a means to apply field-appropriate net normal stress, the determination of volume change as well as water content change (during drying and wetting), and the use of a single specimen for determination of the relationship of soil suction to the volume-mass soil properties. Several research groups have recently developed modified pressure plate-type devices. One such apparatus that allows for testing of the complete SWCC on a single specimen is the modified oedometer (K_o) device (Padilla et al., 2005; Pham et al., 2004). Soil suction is controlled using the axis-translational method, on a pressure plate cell. A K_o SWCC device manufactured by GCTS, Tempe, AZ, is shown in Figures 23 and 24.

Some of the features of the GCTS K_o cell include the simulation of field net normal

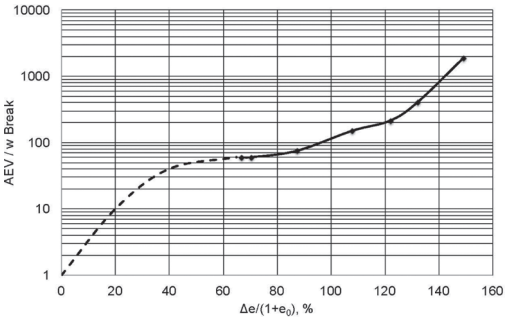

Figure 22. Difference between the break in the gravimetric water content SWCC and the Air-Entry Value for Regina clay.

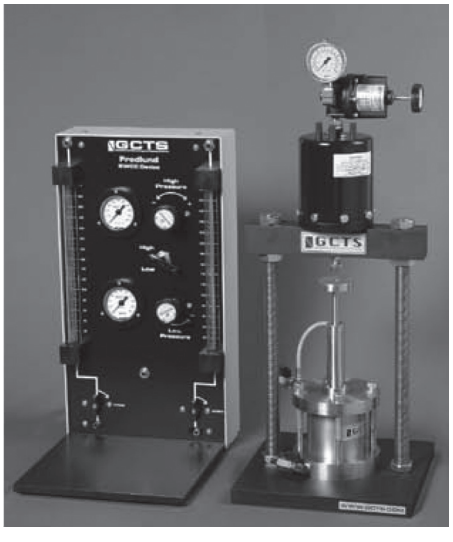

Figure 23. GCTS Pressure plate device.

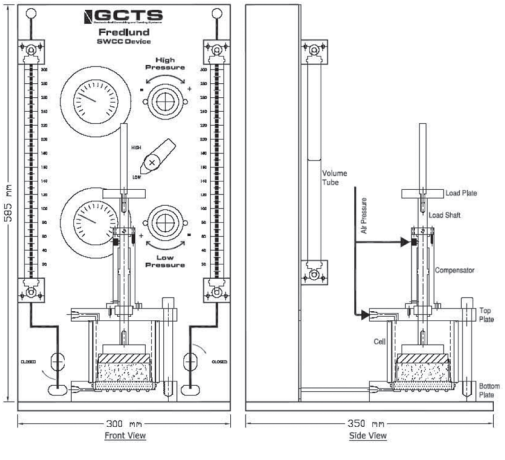

Figure 24. GCTS Pressure plate device.

stress (e.g., overburden plus structural loads), measurement of water released or absorbed from the specimen during the test, capability of tracking the vertical deformation of the soil specimen, and the capability of obtaining several points along the soil-water characteristic curve without dismantling the cell (Perez-Garcia et al., 2008). The ceramic high-air-entry disk, HAED, used in this apparatus is epoxied into a ring that is fitted into a recess on the bottom base plate. The disk has a grooved water compartment to keep the disk saturated and to facilitate the flushing of diffused air. The base has two external ports that connect the water compartment to the drainage system consisting of two graduated volumetric tubes. Each tube has a graduated scale with 1 mm marks. The volume tube measurements can be read to the nearest mm, which translates to accuracy in volume measurements of 0.07 cc. The application of the net normal stress is accomplished with a loading rod inserted from the top of the device and dead weights placed on top of the loading plate. Alternatively, a loading frame can be used to apply loads directly to the loading rod. The application of a vertical load also ensures close contact between the sail specimen and the ceramic disk in addition to more closely simulating field conditions.

A stiff, stainless steel specimen ring is used to constrain the specimen laterally. Compacted or undisturbed specimens with diameters from 50 to 75 mm and 25 mm high can be tested in this device. The platen and the loading rod move up or down with the sample as the sample expands or compresses, and this measurement is tracked with a dial gage or LVDT. A pressure compensator is also provided to null the uplift loads generated when applying pressures inside the cell. The same air pressure applied to the cell is also applied to a piston which has a net area equal to the cross-sectional area of the loading rod.

The axis-translational technique allows the control of negative pore water pressures less than zero-absolute, and consists of elevating the pore-air pressure such that the desired matric suction, $(u_a - u_w)$, is achieved. The saturated HAED used in the axis-translational technique, when saturated, allows the passage of water yet prevents the flow of air up to a value of air pressure corresponding to the air-entry-value of the ceramic disk.

One of the main problems associated with high-air-entry ceramic disk is the diffusion of air that accumulates over time in the water compartment beneath the HAED. For this reason, the device has been designed to allow for flushing air from beneath the HAED. Accumulation of air results in the apparent volume of water coming out of the specimen being larger than actual. If water is going into the sample, diffused air will prevent the water

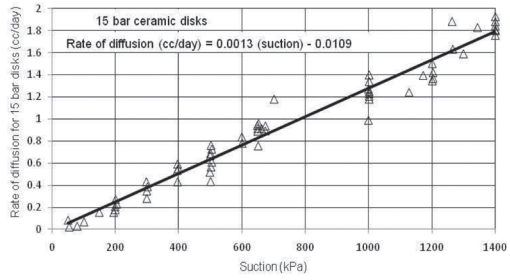

Figure 25. Diffused air through 15 bar high air entry ceramic disks (Padilla et al., 2006).

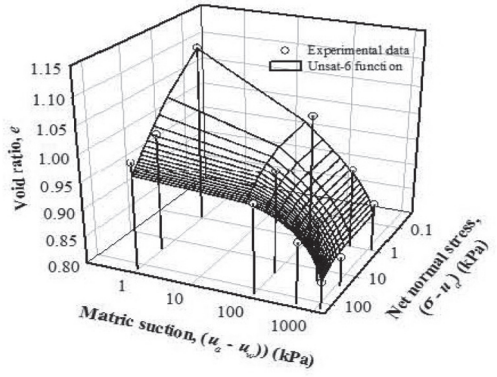

Figure 26. Example of Void Ratio Constitutive Surface for an Expansive Soils Obtained using the GCTS SWCC Device (Singhal, 2010).

from flowing into the specimen if the amount of air is sufficient to retard the water conductivity through the high air entry disk (Padilla et al., 2006). Measured rates of air diffusion as a function of suction for several 15 bar stones are shown in Figure 25. For 15 bar ceramic disks, the diffusion of air at 700 kPa is about 0.9 cc/day and 1.8 cc/day at 1,400 kPa. The amount of diffused air is relatively small when applying low suctions but the rate of air diffusion increases more or less linearly as the air-entry-value of the HAED is approached (Perez, 2006; Perez-Garcia et al., 2008).

An example of the void ratio constitutive surface obtained using the GCTS SWCC device is shown in Figure 26. This surface was obtained along a wetting path, and vertical swell of the specimen was monitored as suction was decreased. The soil classified as a CH, with LL of 82 and PI of 52, and exhibited a medium degree of expansion based on its expansion index (ASTM D 5890–06). Points along the SWCC were obtained for three different net normal stress values, allowing the determination of the constitutive surface. The data

Table 1. Data for Wetting Path for CH soil tested in GCTS SWCC device (Singhal, 2010).

$(u_a - u_w)$ (kPa)	$(\sigma_y - u_a)$ (kPa)	w(%)	S_r(%)	e
1200	1	24.2	76.6	0.890
500	1	26.4	78.6	0.947
100	1	30.3	82.4	1.034
0	1	35.5	88.8	1.126
1200	25	24.8	81.7	0.855
500	25	26.9	83.2	0.910
100	25	30.7	87.6	0.987
0	25	34.5	95.4	1.017
1200	150	25.2	83.5	0.848
500	150	27.1	83.8	0.910
100	150	30.5	89.2	0.963
0	150	32.9	92.7	0.997

points obtained are shown along with the fitted constitutive surface. The fit was obtained using the Unsat-6 function proposed by Vu and Fredlund, 2006. A summary of the data plotted in Figure 26, including degree of saturation data, is provided in Table 1.

It is also possible to obtain the drying SWCC, with volume change determination, using the K_o SWCC device (Singhal, 2010). However, if the confining stress is low, and if the test is begun at a high water content, specimen shrinkage during drying may result in the specimen pulling away from the side walls of the confining ring. There are two effects of specimen shrinkage. One effect is the loss of confinement in the radial direction (K_o conditions no longer apply). Additionally, the SWCC cell must be disassembled and caliper measurements used to obtain radial strains due to shrinkage.

13 BENEFITS AND LIMITATIONS ASSOCIATED WITH ONE-DIMENSIONAL TESTING FOR THE SWCC

An oedometer-type pressure plate apparatus allows for testing of the full SWCC on a single specimen, and does not require cell disassembly at each level of suction considered. Mid-point weighing of the specimen, as required in most pressure plate devices, is not ideal because evaporation of water from the specimen can introduce error. The oedometer-type SWCC cell provides measurements of moisture content change throughout the test without removal of the soil specimen by use of graduated volume tubes, provided evaporation from the graduated tubes in presented or at least accounted for through calibration. It is also helpful for obtaining accurate water content measurements if the SWCC device is kept at relatively stable temperature during testing, as this avoids the development of condensation droplets within the cell that arise from temperature fluctuations. Small differences in water content between direct measurement and volumetric outflow computations at the end of the full SWCC determination, and upon device disassembly, can be adjusted using a correction factor applied to points along the soil-water characteristic curve.

The K_o SWCC device represents an improvement over existing pressure plate devices for geotechnical applications. Net normal stress can be controlled and measurements of volume change can be made during testing to track changes in void ratio and degree of saturation using this device. This is particularly important for geotechnical problems of expansive and collapsible soils.

Void ratio and degree of saturation are not tracked when using conventional pressure plate devices. The general procedure used with the conventional pressure plate device is to have several "duplicate" specimens, and one specimen is removed and weighed to determine water content at each suction value of interest. It is difficult to produce identical specimens unless a compacted soil or a reconstituted soil is being tested. The oedometer apparatus allows the preservation of soil structure in addition to the determination of the SWCC on one specimen. It is likely that sample variability is a greater problem than the potential errors associated with use of "duplicate" specimens and errors associated with mid-point disassembly for obtaining water content measurements.

There are some issues to be addressed and corrections to be made when determining the SWCC relationship using an oedometer-type pressure plate device. The challenges include avoidance of evaporation from water outflow/inflow tubes for long-equilibration time tests, temperature control to minimize or avoid condensation of water inside of the SWCC cell, and determination of volume change during drying if the specimen shrinks from the sidewall of the specimen ring. However, the advantage of the oedometer-type pressure plate device for geotechnical applications are significant. It is important for geotechnical applications to test under appropriate net normal stress and to be able track volume change as soil suction is increased or decreased. It is also important to be able to test specimens for which soil structure is preserved, and this can be done in the K_o pressure plate device. Finally, it is an advantage to be able to develop the full SWCC on one test specimen to avoid variability in the soil specimens.

14 CONCLUSIONS AND RECOMMENDATIONS

Changes in the volume of the soil specimens as soil suction is increased can significantly affect the interpretation of soil-water characteristic curve information. This paper has presented information on the procedures that can be used to properly account for the effects of volume change when interpreting the SWCC for volume change materials. The effects of volume change are shown to be significant, resulting in erroneous calculations of the unsaturated soil property functions.

Laboratory apparatuses have also been described for the measurement of both water volume change as well as overall volume changes. The one-dimensional loading devices may still have the limitation of not being able to measure overall volume change for conditions where the soil specimen separates from the walls of the ring during drying. However, the device can be disassembled after equilibration to each suction to obtain volume change due to shrinkage using micrometer measurements. Studies are needed to determine the effect of net normal stress on radial specimen shrinkage, but it is likely that for many geotechnical applications that sidewall shrinkage may be prevented by the application of net normal (vertical) stress indicative of field conditions.

Following is a summary of the main conclusions from this study.

1. Volume changes associated with an increase in soil suction can significantly affect the determination of the true AEV of the soil.
2. Errors in the determination of the true AEV of an initially slurried clay soil can be several orders of magnitude if volume changes during suction changes are not taken into account.
3. Errors in the determination of the true AEV of a soil can have a significant effect on the estimation of USPFs.
4. The measurement of the shrinkage curve for a soil can be used in conjunction with the gravimetric water content SWCC to determine the true air-entry value for a soil.
5. The true AEV of a soil must be determined from the degree of saturation SWCC.
6. The water storage function can be obtained by differentiating the instantaneous volumetric water content SWCC with respect to soil suction. This is true for suction values less than and greater than the air-entry value of the soil.
7. One-dimensional oedometer apparatuses that can apply controlled soil suctions can provide further insight into the volume-mass behaviour of unsaturated soils.
8. One-dimensional oedometer apparatuses have a limitation in that the soil specimen may pull-away from the confining ring at high soil suctions, particularly when confining stress is low.

The authors would recommend that similar laboratory and parametric type studies be conducted for other volume-mass pathways. Consideration should be given to obtaining the most accurate interpretation of SWCC data for collapsible soils, compacted soils as well as swelling soils.

ACKNOWLEDGEMENTS

The authors desire to acknowledge the equipment development contributions of GCTS, Tempe, AZ, and express our thanks to TOTAL E & P (Canada), for the opportunity to undertake laboratory test results on high volume change Oil Sands tailings.

The authors also wish to acknowledge the assistance of two graduate students in preparing this paper; namely, Elham Bani Hashem, School of Sustainable Engineering and the Built Environment, Arizona State University, Tempe, AZ, supported by the National Science Foundation under Grant No. 1031214. and Fexia Zhang, Department of Civil & Environmental Engineering, University of Alberta, Edmonton, AB, sponsored under NSERC funding. Any opinions, findings, and conclusions or recommendations expressed in this material are those of the authors and do not necessarily reflect the views of the National Science Foundation or NSERC.

REFERENCES

Fredlund, D.G. 1964. Comparison of soil suction and one-dimensional consolidation characteristics of a highly plastic clay. *National Research Council of Canada, Division of Building Research, Technical Report No. 245*, Ottawa, Ontario, Canada.

Fredlund, D.G. 2002. Use of soil-water characteristic curve in the implementation of unsaturated soil mechanics. *UNSAT 2002, Proceedings of the Third International Conference on Unsaturated Soils*, Recife, Brazil, March 10–13, pp. 887–904.

Fredlund, M.D., Wilson, G.W., and Fredlund, D.G. 2002. Representation and estimation of the shrinkage curve. *UNSAT 2002, Proceedings of the Third International Conference on Unsaturated Soils*, Recife, Brazil, March 10–13, pp. 145–149.

Fredlund, D.G. and Rahardjo, H. 1993. *Soil mechanics for unsaturated soils*. John Wiley and Sons New York, N.Y.

Fredlund, D.G. and Xing, A. 1994. Equations for the soil-water characteristic curve. *Canadian Geotechnical Journal*, Vol. 31, No. 3, 521–532.

Fredlund, D.G., Xing, A., and Huang, S.Y. 1994. Predicting the permeability function for unsaturated soils using the soil-water characteristic curve, *Canadian Geotechnical Journal*, Vol. 31, No. 4, pp. 533–546.

Fredlund, D.G., Xing, A., Fredlund, M.D., and Barbour, S. L. 1996. The relationship of the unsaturated soil shear strength to the soil-water characteristic curve, Canadian Geotechnical Journal, Vol. 33, pp. 440–448.

Fredlund, M.D. 2010. User's Manual for SVFlux, Saturated-Unsaturated Numerical Modeling. SoilVision Systems, Saskatoon, Canada.

Padilla, J.M., Perera, Y.Y., Houston, W.N., and Fredlund, D.G. 2005. A new soil-water characteristic curve device. Proceedings of Advanced Experimental Unsaturated Soil Mechanics, An International Symposium, EXPERUS 2005, Trento, Italy, June 27–29, pp. 15–22.

Padilla, J.M., Perera, Y.Y., Houston, W.N., Perez, N., and Fredlund, D.G. 2006. Quantification of air diffusion through high air entry ceramic disks. *Proceedings of the Fourth International Conference on Unsaturated Soils*. Arizona, 1852–1863

Perez, N. 2006. Development of a protocol for the assessment of unsaturated soil properties. *PhD dissertation*. Arizona State University.

Perez-Garcia, N., Houston, S. Houston, W., and Padilla, M., 2008. An odedometer-type pressure plate SWCC apparatus, ASTM Geotechnical Testing Journal, Vol 31, No. 2, pp 115–123.

Pham, H., Fredlund, D.G., and Padilla, J.M. 2004. Use of the GCTS apparatus for the measurement of soil-water characteristic curves. Proceedings of the 57th Canadian Geotechnical Conference, Quebec City, Quebec, Oct. 24–27, pp. 1–6.

Singhal, S. 2010. Expansive Soil Behavior: Property Measurement Techniques and Heave Predction Methods. Ph.D. Disseration, Arizona State University, Tempe, AZ, USA.

Van Genuchten, M.T. 1980. A closed-form equation for predicting the hydraulic conductivity of unsaturated soils. Soil Science Society of America Journal, Vol. 44, pp. 892–898.

Vanapalli, S.K., D.G., and Pufahl, D.E. 1996. The relationship between the soil-water characteristic curve and the unsaturated shear strength of a compacted glacial till, *Geotechnical Testing Journal, ASTM*, Vol. 19, No.2, pp. 259–268.

Vu, H.Q. and Fredlund, D.G. 2006. Challenges to modeling heave in expansive soil, *Canadian Geotechnical Journal*, Vol. 43, pp. 1249–1272.

This page intentionally left blank

Advances in Unsaturated Soils – Caicedo et al. (eds)
© 2013 Taylor & Francis Group, London, ISBN 978-0-415-62095-6

Ventilation effects in an argillaceous rock tunnel examined via unsaturated soil mechanics

A. Gens
Universitat Politècnica de Catalunya (Barcelona Tech), Barcelona, Spain

B. Garitte
CIMNE—Universitat Politècnica de Catalunya (Barcelona Tech), Barcelona, Spain

ABSTRACT: The paper presents the observations, analysis and interpretation of a long-term ventilation test performed in the Mont Terri underground laboratory. An unlined 1.3 m diameter tunnel excavated in Opalinus clay has been subjected to two controlled ventilation periods. Extensive instrumentation has provided observations concerning relative humidity, pore pressures and displacements in the rock. In addition, boreholes have been drilled at several times during the experiment to obtain independent measurements of water content and degree of saturation of the rock. It has been found that an unsaturated zone surrounding the tunnel, though small in extent, largely controls the progress of drying and other effects associated with ventilation. The interpretation of the test has been based on a coupled multi-phase hydromechanical numerical model in which unsaturated soil mechanics concepts such as vapour diffusion, relative permeability and retention curve play a paramount role.

1 INTRODUCTION

All tunnels are subjected to ventilation to a greater and lesser extent, both during construction and during operation. Argillaceous hard soils and soft rocks are potentially sensitive to ventilation effects; ventilation may cause some degree of damage leading to cracking and permeability increases and may also trigger chemical processes such as pyrite oxidation and gypsum precipitation that, in turn, can also have hydromechanical effects.

Those potential effects are quite important in the context of using argillaceous materials as host rocks for geological disposal of radioactive waste. In particular, damage and hydromechanical variations in the zone adjacent to the tunnel is directly relevant to the safety of the repository as it may provide a preferential pathway for the migration of radionuclides. It is therefore necessary to examine those potential effects in detail, preferably under realistic conditions.

In this paper, the observations gathered during a field-scale ventilation test carried out in the Mont Terri underground laboratory are examined and interpreted assisted by the performance of coupled hydromechanical numerical analyses. Because of the nature of a ventilation test (that may lead to desaturation of the host material), the numerical computations must be based on a formulation firmly grounded in the concepts and approaches of unsaturated soil mechanics.

2 DESCRIPTION OF THE TEST

The Ventilation Test (VE) has been performed in a 10 m section of a 1.3 m diameter unlined microtunnel excavated in the Mont Terri underground laboratory (Figure 1).

The Mont Terri laboratory (Thury & Bossart 1999) has been excavated in Opalinus clay, a stiff overconsolidated clay of Lower Aalenian age (Middle Jurassic) found in the Jura mountains of Northern Switzerland. There are three slightly different facies containing different mineral proportions: a shaly facies in the lower part of the deposit, a 15 m thick sandy-silty facies in the centre and a sandy facies interstratified with shaly facies in the upper part. The content of clay minerals may range from 40% to 80%, depending on the facies. The clay was sedimented in marine conditions, it is very strongly bedded and its total thickness is about 160 m. In the location of the Mont Terri laboratory, overburden varies between 250 and 320 m. The laboratory is situated in an asymmetrical anticline formed during the folding of the Jura Mountains. As a result, the rock strata dip with an angle of 25°–45° to the southeast. Information on the properties of Opalinus clay has been reported in Bock (2001), Wileveau (2005), Gens (2012).

The microtunnel was excavated in 1999 in the shaly facies, parallel to the New Gallery, using the raise-boring technique. This direction is perpendicular

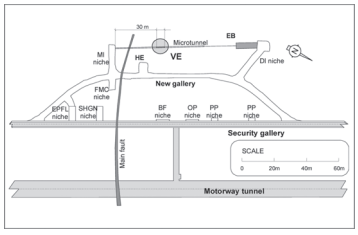

Figure 1. Location of the microtunnel where the VE experiment was performed. Mont Terri underground laboratory.

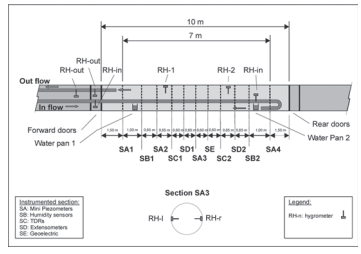

Figure 2. Lay out of the Ventilation test (VE).

to the bedding trace that dips at an angle of 25° towards the SE at this location.

The layout of the VE test is shown in Figure 2. The 10 m section was sealed off by means of two double doors made of exotic wood insensitive to relative humidity (RH) variations (Figure 3). The controlled ventilation during the test was achieved using a system consisting of a blowing device, located outside the test section. It included a compressor, a drier and a bubbler, as well as inflow and outflow pipes equipped with flowmeters, hygrometers and thermometers. Measurement of airflow mass and relative humidity of ingoing and outgoing air allowed establishing the global water mass balance of the test section, as reported below. More details are given in Mayor & Velasco (2008).

Several phases in the history of the test can be distinguished (Figure 4):

- Phase 0 in which the VE tunnel was excavated and left open without controlled ventilation conditions from February 1999 to July 2002. This phase lasted 41 months.
- Phase 1 in which the VE tunnel was subjected to controlled ventilation conditions. During the first stage (from July 8, 2002 to May 28, 2003), the RH in the tunnel was allowed to be close to 100% causing some resaturation of the rock. In the second stage (from May 28, 2003 to January 29, 2004) ventilation with controlled RH was applied. Three RH steps were applied: 80%, 30% and 2%. This Phase lasted about 19 months (11 months for the first stage and 8 months for the second).
- Phase 2 consisted also of two stages. In the first stage (from January 29, 2004 to July 11, 2005), RH was again allowed to be close to 100% causing some resaturation of the host rock. Afterwards, a controlled ventilation stage was performed (from July 11, 2005 to September 24, 2006). In this stage the RH of the incoming air was kept at the low value of 2% to ensure the strongest possible ventilation effects over the time available for the test. In total, this phase lasted 32 months, 12 months for the first stage and 21 months for the final strong ventilation stage.

Figure 3. Ventilation test section.

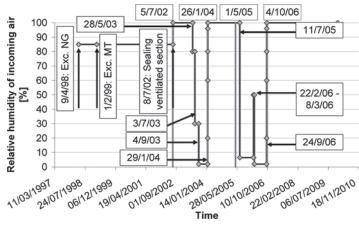

Figure 4. Timeline of the Ventilation test (VE) tunnel section.

The relative humidity values before the start of measurements is an estimation based on the backanalysis of the pore water pressures in the rock when monitoring started. During the test, the nominal relative humidity values of Figure 4 were not exactly achieved; the relative humidity values actually measured inside the tunnel and in a sensor 2 cm inside the rock are shown in Figure 5.

Between May to July 2002, a 2 m radius around the test section was instrumented with hygrometers for the measurement of relative humidity (RH), piezometers and extensometers. Some additional hygrometers and piezometers were installed before the desaturation stage of Phase 2. In addition, several drilling campaigns were also carried out at several stages of the experiment to determine the water content around the microtunnel. The times of the drilling campaigns are indicated by vertical dotted lines in Figure 5.

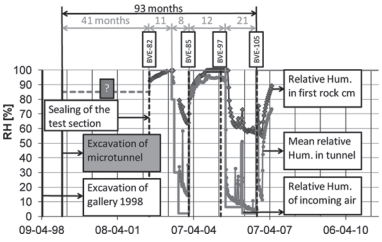

Figure 5. History of the relative humidity in the incoming air, inside the tunnel (mean) and measured in a sensor 2 cm inside the rock. Vertical dotted lines indicate the times of the various drilling campaigns.

3 HYDROMECHANICAL FORMULATION

The hydromechanical (HM) formulation used is a particular case of the general THM formulation developed in Olivella et al. (1994). The key equation in this particular case is the water mass balance (Garitte et al., 2010) expressed as:

$$\frac{\partial}{\partial t}(\theta_l^w S_l \phi + \theta_g^w S_g \phi) + \nabla \cdot (\mathbf{j}_l^w + \mathbf{j}_g^w) = f^w \tag{1}$$

where the first terms reflects the change of water mass with time in a generic representative volume and the second term represents the divergence of water flow. The right hand side term is a sink/source term that is equal to 0 in the present case. θ_l^w and θ_g^w are the volumetric masses of water in the liquid and the gas phase, respectively. $\theta_l^w = \omega_l^w \cdot \rho_l$, where $\omega_l^w = m_w/m_l$ is the mass fraction of water in the liquid. The same nomenclature is used for the gas phase. S_l and S_g are the degrees of saturation of liquid and gas phases, respectively. j_l^w and j_g^w are the fluxes of water (with respect to a fixed reference) in the liquid and gas phases, respectively.

The advective flow of water in the liquid phase j_l^w [kg/m^2/s] is:

$$j_l^w = \theta_l^w \cdot \mathbf{q}_l \tag{2}$$

where q_l [m/s] is the Darcy velocity that is proportional, to the water potential gradient:

$$\mathbf{q}_l = -\frac{\mathbf{k} k_{rl}}{\mu_l}(\nabla P_l - \rho_l \mathbf{g}) \tag{3}$$

where $\boldsymbol{k}$ is the intrinsic permeability [m^2], μ_l is the dynamic viscosity [Pa.s], k_{rl} is a coefficient depending on the degree of saturation (or suction), P_l is the liquid pressure, ρ_l is the liquid density [kg/m^3] and $\mathbf{g}$ is the gravity acceleration [m/s^2].

A critical relationship is the dependence of the permeability on the degree of saturation. It is introduced through the expression:

$$k_{rl} = \sqrt{S_l}(1-(1-S_l^{1/\lambda})^{\lambda})^2 \tag{4}$$

known as Van Genuchten law, where λ is a shape parameter.

The transport of water in the gas phase can be decomposed in:

$$j_g^w = (i_g^w)_{advection} + (i_g^w)_{diffusion} + (i_g^w)_{dispersion} \tag{5}$$

in which the first term represents the flux of water by motion of the gas phase and the second term the flux of water by diffusion of water vapour inside the gas phase (non-advective flow). Dispersion has been neglected.

Vapour diffusion is expressed by Fick's law:

$$(i_g^w)_{diffusion} = -(\phi \rho_g S_g D_g^w \mathbf{I}) \nabla \omega_g^w \tag{6}$$

where D_g^w [m^2/s] is the vapour diffusion coefficient and $\nabla \omega_g^w$ is the gradient of vapour concentration. Although gas motion was found to be negligible, vapour diffusion turned out to have a significant influence on the results.

The relationship between suction ($p_g - p_l$) and the liquid degree of saturation is modelled by the Van Genuchten retention curve:

$$S = \frac{S_l - S_{rl}}{S_{ls} - S_{rl}} = \left(1 + \left(\frac{p_g - p_l}{P}\right)^{\frac{1}{1-\lambda^*}}\right)^{-\lambda^*} \tag{7}$$

where λ^* is a shape parameter, S_{rl} is the residual saturation, S_{ls} is the maximum saturation. P is the air entry value.

Finally, Kelvin's law relates vapour concentration in the gas phase to water potential (suction):

$$\theta_g^w = \omega_g^w \cdot \rho_g = (\theta_g^w)^0 \cdot \exp\left[\frac{\psi \cdot M_w}{R \cdot (273.15 + T) \cdot \rho_l}\right] \tag{8}$$

M_w is the molecular mass of water, R the universal gas constant and ψ is the total potential of the water that in this case coincides with the matric suction (gas pressure is assumed atmospheric and osmotic suction is not considered). The relative humidity (RH) is defined as the ratio of the partial pressure of water vapour in the mixture to the saturated vapour pressure of water at a given temperature. It can be related to θ_g^w through:

$$RH = \frac{p_v}{(p_v)_0} \cdot 100 = \frac{\theta_g^w}{(\theta_g^w)_0} \cdot 100 \tag{9}$$

where p_v is the vapour pressure and subscript $()^0$ stands for the saturated state.

4 MODEL FEATURES AND PARAMETERS

4.1 *Model features*

A plane strain domain representative of the central section of the ventilation test length was adopted for performing the coupled hydromechanical analyses required for the interpretation of the test (Figure 6). Both the ventilation test and the parallel New Gallery are present in the mesh. Initial pore water pressure distribution was taken as hydrostatic, reaching a value of 1.85 MPa at the microtunnel level (Bossart et al., 2004, Croisé et al., 2004). The stress state is isotropic and its initial distribution is geostatic and equal to 4.9 MPa at the microtunnel level, the mean value suggested by Martin and Lanyon (2003). Because the microtunnel is perpendicular to the bedding trace and bedding dip angle is small (25°), it is reasonable to assume anisotropy of permeability in the conceptual model using a higher permeability value in the horizontal plane that corresponds approximately to the bedding plan. Water flow due to osmotic gradients was found to have a negligible effect on results (Garitte & Gens 2007) and it is not considered in this paper. The hydromechanical history prior to the start of the Ventilation test (excavation of the New Gallery, excavation of the microtunnel and the subsequent Phase 0 period) was simulated to provide realistic initial conditions.

The key boundary condition, however, is the hydraulic condition at the tunnel surface boundary. It is known that the average value of RH of the air is different from the RH of the rock close to the interface because of a complex set of phenomena often grouped under the name of skin effect. In the analyses, the concentration of vapour is prescribed at the tunnel wall via the following expression:

$$j_g^w = \beta_g \left(\left(\rho_g \omega_g^w \right)^0 - \left(\rho_g \omega_g^w \right) \right) \tag{10}$$

where j_g^w [kg/s/m^2] is the flux of water in the gas phase, the subscript $()_0$ stands for the prescribed values, ρ_g [kg/m^3] is the gas density, ω_g^w is the mass fraction of water and gas and β_g [m/s] is a coefficient that controls the velocity at which the boundary values tend towards the prescribed values. For low β_g values, equilibrium is not reached instantaneously and water is extracted more slowly. Note that, in accordance with equation (9), applying vapour concentration is equivalent to prescribing relative humidity. In the analyses, the values of β_g have been selected in order to obtain a good agreement with the RH values measured in a sensor in the rock located at 2 cm from the tunnel wall during Phase 1. The values used have been 1E-3 for desaturation phases and 6E-3 in the resaturation phases. The same values have been retained for the analysis of Phase 2. The calculations have been performed using the CODE_BRIGHT simulator (Olivella et al., 1996).

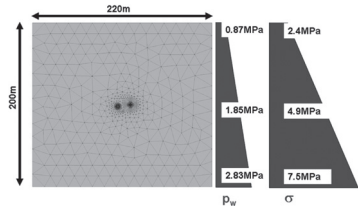

Figure 6. Model domain used in analysis showing initial conditions.

4.2 *Parameters*

The parameters adopted for the analysis are based on some reference works (Bock 2001, Gens et al., 2007) and on some additional information specific to the VE project (Mayor and Velasco 2008). The main ones are listed in Table 1.

Moreover, a laboratory drying experiment was set up before the start of the in situ VE (Floria et al., 2002). Three Opalinus Clay samples were placed on balances in a drying chamber. All sample walls, except the top, were isolated in order to create conditions as close as possible to 1D flow. The measured water losses in the three samples are presented in Figure 7. After 142 days, sample A had lost about 150 gr from the initial 300 gr of water. Simulations were run to calibrate some parameters and to validate the formulation. These simulations showed the importance of i) the value of water permeability and its dependency on degree of saturation and ii) water transport through vapour diffusion. The first step of the calibration consisted in fitting the first days of the experiment to obtain the saturated permeability. The remaining time of the experiment is then used to calibrate the dependency of permeability on degree of saturation (equation 4), a key aspect of the formulation. The influence of the saturation dependency of permeability is illustrated in Figure 7, where λ is the shape parameter of the permeability—saturation relationship. For a value of one, permeability is constant and equal to the saturated value. For lower values of λ, permeability decreases with degree of saturation, the reduction being faster the lower the λ value is. As indicated by Figure 7, a value close to $\lambda = 0.5$ provides a good representation of the drying results. An additional simulation was run in which vapour diffusion was neglected. In this case, an unrealistic increase of the permeability by a factor of three was necessary to keep a good fit of the water loss, demonstrating the importance of water transport in vapour form.

Table 1. Main Opalinus clay parameters.

Parameter	Value
Porosity	0.162
Intrinsic permeability (parallel and perpendicular)	$7 \cdot 10^{-20}$ m^2 $1.4 \cdot 10^{-20}$ m^2
Liquid relative permeability, λ	0.52
Vapour diffusion coefficient	$2.7 \cdot 10^{-5}$ m^2/s
Young modulus	7000 MPa
Poisson coefficient	0.2
Friction angle	19.3°
Cohesion	1.2 MPa
Biot coefficient	0.6
Air entry value*	11 MPa
Surface tension*	$7.2 \cdot 10^{-2}$ N/m
Shape parameter*	0.29

* Retention curve parameters.

As it is often the case in unsaturated soil mechanics, the retention curve was also shown to have a significant influence on the results. Its parameters (Table 1) were determined based on the results of several experimental investigations (Gens 2000, Muñoz et al., 2003, Zhang & Rothfuchs 2005, Villar, 2007). Figure 8 shows the retention curve adopted. Porosity was chosen such that the water content of the saturated material is equal to 7.14% corresponding with the undisturbed water content of saturated Opalinus clay in the vicinity of the microtunnel (averaged from the different drilling campaigns). Permeability was taken anisotropic, with a lower value perpendicular to the bedding plane as suggested by the pattern of pore water pressure observations. Mohr-Coulomb strength parameters were determined using triaxial laboratory tests performed by Schnier (2005).

5 INTERPRETATION OF THE RESULTS

5.1 *Boundary condition and global water balance*

As stated above, there are significant differences between the relative humidity of the incoming air (prescribed) and the relative humidity measured in the tunnel and even larger differences with the relative humidity measured in a sensor placed 2 cm inside the rock. Hence, the value of the parameter β_g of the hydraulic boundary condition was adjusted to account for this difference using the measurements of phase 1. As shown in Figure 9, it has been possible in this way to reproduce satisfactorily the evolution of the relative humidity close to the surface of the tunnel, an essential requirement for a subsequent successful representation of the test results. It should be noted that the results obtained for Phase 2 are purely predictive.

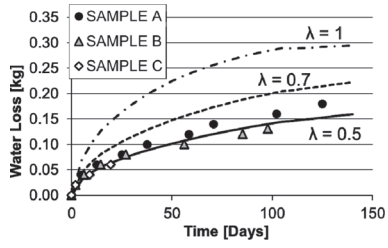

Figure 7. Water extracted in the laboratory drying test (three specimens).

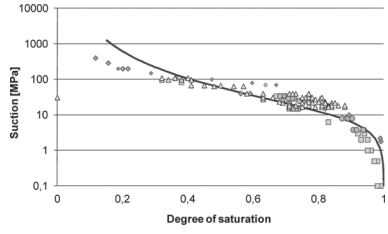

Figure 8. Retention curve used in the analyses.

The ventilation system includes an air blowing device, with monitored air flow, temperature and air relative humidity on entry and exit. This allows the calculation of the water mass balance of the test section. Using the rock parameters and the hydraulic boundary condition determined as described before, an excellent simulation of the amount of water extracted from the test section is achieved (Figure 10). A parametric study of the in situ case also showed the important influence of the permeability value and its dependency on saturation. Vapour diffusion was found to be somewhat less significant than in the laboratory drying experiment but certainly not negligible. The reason probably lies in the fact that, in the tunnel, water from the rock mass is available to partially replace the evaporation water losses causes by ventilation.

5.2 *Evolution of relative humidity in the rock*

In phase 1, the relative humidity in the rock mass was monitored by hygrometers placed between 30 cm and 2.15 m from the tunnel wall. Before the experiment the likely position of the saturation limit was assumed to be in that range, but it turned out to be an overestimation. Indeed, in that range, all hygrometers provided readings above 95% which is outside the confidence limit of these devices. As a result, before phase 2, new hygrometers were installed in the 30 cm adjacent to the tunnel wall allowing a much better characterization of the evolution and distribution of relative humidity of the rock in response to ventilation.

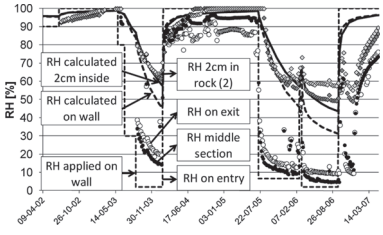

Figure 9. Evolution of the relative humidity in the incoming air, inside the tunnel and in a sensor 1 cm inside the rock. Observed and computed results.

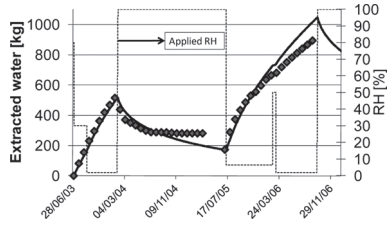

Figure 10. Water extracted from the test section. Observed and computed results.

Figure 11 shows the observed and the computed results of the evolution of relative humidity for the sensors emplaced before the desaturation stage of Phase 2. It can be seen that the measured evolution of relative humidity is closely matched by the numerical model with the exception of the overestimation of the drying in the rock in the sensor placed 7 cm distance from the wall (r = 0.72 m).

5.3 *Distributions of relative humidity, water content and degree of saturation in the rock*

The distributions of the relative humidity with distance to the tunnel wall are shown in Figures 12a for the end of Phase 1 desaturation and in Figure 12b for the end of the stronger Phase 2 desaturation. It can be noted that relative humidity is clearly below 100% only in the 40–50 cm close to the tunnel. It is also apparent that the model closely reproduces the measured distribution. It can be noted that two model results have been plotted corresponding to different line orientations. They are slightly different because of the assumed anisotropy in permeability. Examination of the precise distribution of relative humidity close to the tunnel surface was only possible in Phase 2 where more hygrometers had been added at short distances from the tunnel wall. A close-up of Figure 12b is presented in Figure 13, confirming the good representation of the relative humidity distribution by the numerical model.

In Figure 12, the measured pore pressures in the various piezometers placed in the rock are

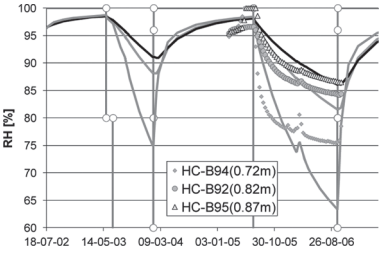

Figure 11. Evolution of relative humidity in the rock at 7 cm (r = 0.72 m), 17 cm (r = 0.82 m) and 22 cm (r = 0.87 m) distance from the tunnel wall.

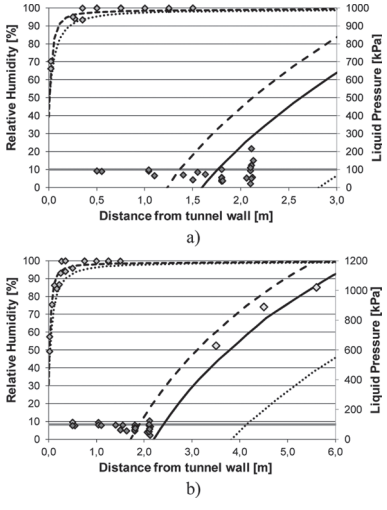

Figure 12. Distribution of relative humidity and pore pressures in the rock. Observations and model results (dashed lines: vertical direction, dotted lines: horizontal direction, full line: 45° direction). a) At the end of Phase 1 desaturation period. b) At the end of Phase 2 desaturation period.

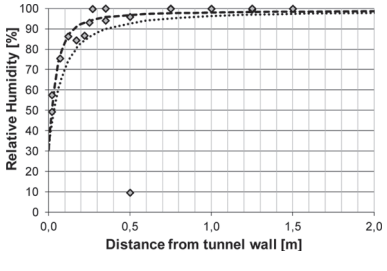

Figure 13. Distribution of relative humidity in the rock close to the tunnel wall. Observations and model results (dashed lines: vertical direction, dotted lines: horizontal direction).

also shown together with the model computations again along different line orientations. It is apparent that for distances below 2–2.5 m the rock

is under suction; this is why all piezometers read atmospheric pressure. However, the piezometers at longer distances from the tunnel, installed after Phase 1, record positive values of pore pressures that are in fact in quite good agreement with model results (Figure 12b).

As mentioned above, boreholes were drilled at different times during the Ventilation Test in order to obtain direct measurements of water content at different distances from the tunnel. Figure 14a shows the water contents obtained at the end of Phase 2 desaturation stage. The average initial water content of the rock (7.14%) is also indicated in the Figure. It should be noted that drilling was accomplished about 10 days after finishing ventilation, but only very slight water content changes have taken place in such a short period that, in any case, has been taken into account in the modelling. It is apparent that this totally independent data confirm the fact that desaturation has only taken place in the 40–50 cm adjacent to the tunnel wall. Figure 14b presents the same data in terms of degree of saturation showing that in the rock adjacent to the tunnel degree of saturation fall down to values of 50%–60%. It is also noteworthy, that the numerical model provides a good representation of the test results in terms of water content and degree of saturation.

Taking into account all those results, it is useful to distinguish two different zones around the tunnel for characterizing the effects of ventilation.

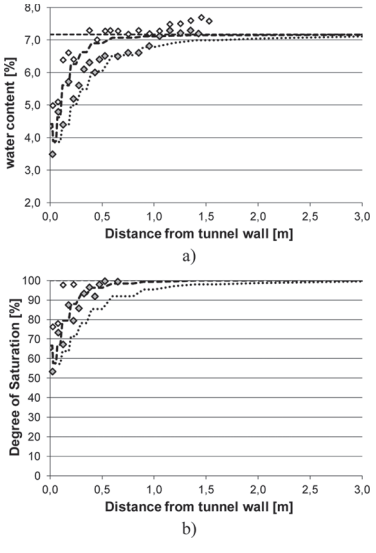

Figure 14. Distribution of water content and degree of saturation in the rock at the end of Phase 2 desaturation. Observations and model results (dashed lines: vertical direction, dotted lines: horizontal direction).

There is a limited zone (maximum thickness about 50 cm) where the material becomes unsaturated and a larger zone (extending to about 2.5–3 m from the tunnel wall) where the material is under suction but still saturated. Naturally, Opalinus clay, being a fine-grained material, can sustain significant suction values without becoming unsaturated. It is interesting to note (Garitte and Gens, 2012) that the suction zone already extended to about 2 m before the start of the ventilation test; so it has been extended only moderately by strong ventilation.

5.4 *Displacements*

Although it is expected that ventilation will generate small displacements only (especially if compared with excavation movements), extensometers were installed in the test section. Figure 15 shows the measured relative displacements between the tunnel wall and an anchor point 2 m inside the rock mass. The relative humidity of the incoming air is also plotted for reference. A clear pattern emerges: each wetting period induces an expansion of the rock mass around the tunnel whereas drying causes compression. The simulation represents quite well this tendency that is basically due to the changes in suction during the drying-wetting cycles. In any case, the magnitude of the displacements induced by the wetting—drying cycles is, as anticipated, small.

6 CONCLUSIONS

The long-term controlled ventilation test performed at the Mont Terri underground laboratory has provided abundant data to examine the potential effects of ventilation in tunnels constructed in argillaceous rock. The field test results have been interpreted using a numerical model capable of simulating the relevant processes and the significant features involved in the test.

Two different zones around the tunnel have been identified: a desaturation zone and a larger zone in which the argillaceous rock is under suction. The desaturation zone reaches only about 50 cm inside the rock in spite of the very low relative humidity applied during ventilation. The suction zone extends to 2.5–3 m away from the tunnel wall but it appears that it has only been moderately enlarged by ventilation.

A coupled hydromechanical numerical model, based on a multi-phase formulation, has been able to reproduce successfully the pattern of observations of the test, both qualitatively and quantitatively. Critical features of the model are a realistic representation of vapour movement and the adoption of a hydraulic boundary condition on the tunnel wall capable of accounting for skin effects.

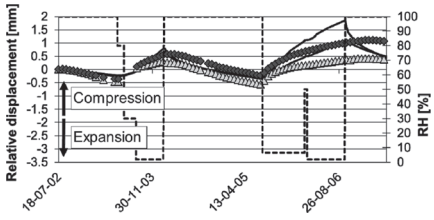

Figure 15. Relative displacement between the tunnel wall and an anchor point 2 m inside the rock mass. Observed and computed results.

It is important to realize that, although the unsaturated zone is small in extent, it largely controls the progress of drying and other effects associated with ventilation. Therefore, features such as the relationship of relative permeability with suction, the retention curve or vapour diffusion play a key role in a proper study of the test. Consequently, unsaturated soil mechanics concepts are essential for a satisfactory interpretation and understanding of the test and, more generally, of ventilation effects in tunnels excavated in argillaceous media.

ACKNOWLEDGEMENTS

This work was supported by the European Commission through NF-PRO project (Contract F16 W-CT-2003-02389). The authors are also grateful for the support of ENRESA and the Mont Terri Project and for the useful discussions with Juan Carlos Mayor and Manuel Velasco. The contribution of the Ministry of Science and Innovation of Spain through grant BIA2011-27217 is gratefully acknowledged too.

REFERENCES

Bock, H. 2001. RA Experiment. Rock Mechanics analyses and synthesis: Data Report on Rock Mechanics. Technical Report 2000–02. Mont Terri Project.

Bossart, P., Meier, P.M., Moeri. A., Trick, T. & Mayor, J.-C. 2004. Structural and hydrogeological characterisation of the excavation-disturbed zone in the Opalinus Clay (Mont Terri Project, Switzerland). *Applied Clay Science* 26: 429–448.

Croisé, J., Schlickenrieder, L., Marschall, P., Boisson, J.-Y., Vogel, P. & Yamamoto, S. 2004. Hydrogeological investigations in a low permeability claystone formation: the Mont-Terri Rock Laboratory. *Physics and Chemistry of the Earth* 29: 3–15.

Floría, E., Sanz, F.J. & García-Siñeriz, J.L. 2002. Drying test: evaporation rate from core samples of "Opalinus clay" under controlled environmental conditions. Deliverable D6, VE project (FIKW-CT2001–00126).

Garitte, B. & Gens, A. 2007. Modelling and Interpretation of the Ventilation Experiment: HM-C mechanisms in Opalinus clay. Final Activity Report. NF-PRO Project, Deliverable D 4.3.23 (F16 W-CT-2003–02389).

Garitte, B. & Gens, A. 2012. The response of an argillaceous rock to ventilation: process identification and analysis of an in situ experiment. In Qian & Zou (eds): *Harmonizing Rock Engineering and the Environment*: 634–639. London: Taylor & Francis Group.

Garitte, B., Gens, A., Liu, Q., Liu, X., Millard, A., Bond, A., McDermott, C., Fujita T. & Nakama, S.. 2010. Modelling benchmark of a laboratory drying test in Opalinus Clay. In Zhao, Labiouse, Dudt & Mathier (eds), *Rock Mechanics in Civil and Environmental Engineering*: 767–770, Taylor & Francis Group.

Gens, A., 2000. *HE Experiment: complementary rock laboratory tests*. Technical Note TN 2000-47. Mont Terri Project.

Gens, A. 2012. On the hydromechanical behaviour of argillaceous hard soils-weak rocks. In A. Anagnostopoulos et al. (Eds.), *Proceedings of the 15th European Conference on Soil Mechanics and Geotechnical Engineering, Athens.* IOS Press.

Gens, A., Vaunat, J., Garitte, B. & Wileveau, Y. 2007. In situ behaviour of a stiff layered clay subject to thermal loading: observations and interpretation. *Géotechnique* 57: 207–228.

Martin, C.D. & Lanyon, G.W. 2003. Measurement of in-situ stress in weak rocks at Mont Terri Rock Laboratory, Switzerland. *International Journal of Rock Mechanics & Mining Science* 40: 1077–1088.

Mayor, J.C. & Velasco, M. 2008. *The Ventilation Experiment Phase II (Synthesis report)*. NF-PRO Project, Deliverable D 4.3.18 (F16 W-CT-2003-02389).

Muñoz, J.J., Lloret, A. & Alonso, E. 2003. Laboratory Report: Characterization of hydraulic properties under saturated and non saturated conditions, Project Deliverable D4, VE project (FIKW-CT2001-00126).

Olivella, S., Carrera, J., Gens, A. & Alonso, E.E. 1994. Non-isothermal Multiphase Flow of Brine and Gas through Saline media. *Transport in porous media* 15: 271–293.

Olivella, S., Gens, A., Carrera, J. & Alonso, E.E. 1996. Numerical formulation for a simulator (CODE-BRIGHT) for the coupled analysis of saline media. *Engineering Computations* 13: 87–112.

Schnier, H. 2005. LT experiment: Strength tests on cylindrical specimens, documentation and evaluation, (Phases 6 and 7). Mont Terri Project: Technical Note, TN 2002–50.

Thury, M. & Bossart, P. 1999. The Mont Terri rock laboratory, a new international research project in a Mesozoic shale formation, in Switzerland. *Engineering Geology* 52 (3–4): 347–359.

Villar, M.V. 2007. Retention curves determined on samples taken before the second drying phase. Technical report M2144/5/07. Madrid: CIEMAT.

Wileveau, Y. 2005. *THM behaviour of host rock (HE-D) experiment: Progress report. Part 1*. Technical Report TR 2005-03. Mont Terri Project.

Zhang, C.L. & Rothfuchs, T. 2005. *Report on instrument layout and pre-testing of large lab VE-tests*. NF-PRO Project, Deliverable 4.3.11 (F16 W-CT-2003-02389).

Advances in Unsaturated Soils – Caicedo et al. (eds)
© 2013 Taylor & Francis Group, London, ISBN 978-0-415-62095-6

Compacted soils: From physics to hydraulic and mechanical behaviour

S. Leroueil
Department of Civil and Water Engineering, Université Laval, Québec, QC, Canada

D.W. Hight
Geotechnical Consulting Group, London, UK

ABSTRACT: Due to the improvements in our knowledge of unsaturated soil mechanics and in the measurement of soil suction, our understanding of compacted soils has improved considerably. The paper describes the physics that underlies the behaviour of compacted soils and its implications in terms of the hydraulic and mechanical behaviour of compacted soils. A resulting conceptual model is presented. Reference is made to practical implications.

1 INTRODUCTION

Compaction of soils is one of the most common activities in geotechnical engineering. However, it is generally recognised that the behaviour of compacted soils is complex and, when it comes time to specifying compaction conditions for earthworks or to predict the behaviour of compacted soils, the geotechnical engineer is often perplexed. In recent years, however, the development of unsaturated soil mechanics and of technologies allowing for testing of unsaturated soils and measurement of suction have significantly improved our understanding of the behaviour of compacted soils. This paper aims to explain the physics that underlies the behaviour of compacted soils and to assess its implications in terms of hydraulic and mechanical behaviour when the soil is as-compacted, submerged and saturated. Aspects related to drying are not considered. Reference is made to some practical implications.

2 PHYSICS OF COMPACTED SOILS

Compaction is the densification of soils by application of mechanical energy to expel air. In the laboratory, compaction can be performed statically, dynamically (by impacts) or by kneading. If a soil is compacted at different water contents with a given type and amount of compaction effort, a compaction curve relating the soil's dry density to its compaction water content can be drawn. As illustrated in Figure 1, the dry density (or dry unit weight) increases to a maximum value and then decreases as the compaction water content increases. The water content at which the maximum dry density is reached is the optimum water content w_{opt}. On the same diagram, lines of equal degree of saturation can also be drawn as they depend only on soil particle density ρ_s. For the examples shown in Figure 1, the optimums correspond to a degree of saturation of about 72%. It can also be noted that the compaction curves never reach the 100% degree of saturation curve, which means that some air remains trapped in the soil.

The bases of the compaction test were established by Proctor (1933) who expressed the relationship between compaction energy, water content and the resulting dry density in the form of the so-called compaction diagram. It is generally recognised that the compaction curve depends on the soil, the mode of

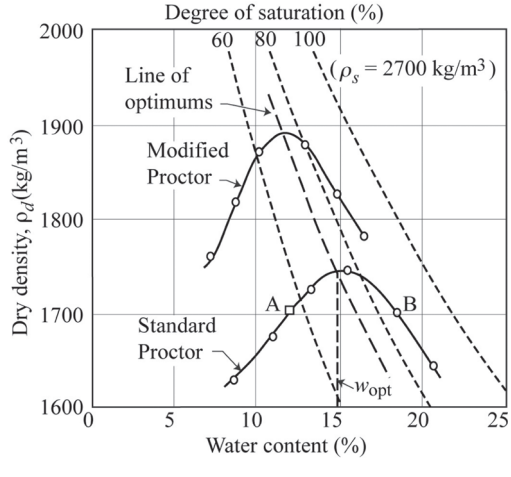

Figure 1. Compaction curves obtained in Standard proctor and Modified Proctor compaction tests performed on the same soil (fictitious data).

compaction and the energy provided. As for the shape of the compaction curve, it has been attributed to the lubricating effect of water that facilitates the arrangement of soil particles as water content increases, and explains the initial increase in dry density towards the maximum. However, as water content increases beyond the optimum, the relative volume of water increases and the dry density decreases. As will be shown later, an important factor influencing the dry density and fabric created by compaction is suction.

The most common compaction test is the Standard Proctor compaction test (ASTM D698-12) corresponding to an energy of 600 kN.m/m^3. The Modified Proctor compaction test (ASTM D1557-12) involves an energy that is 4.5 times larger. As indicated in Figure 1, this results in a higher maximum dry density at a lower optimum water content. However, the degree of saturation at the optimum is not very different and the "line of optimums" is essentially a line of constant degree of saturation $S_{r\text{-}opt}$, of about 72% on the figure. A soil compacted to a degree of saturation larger than that at the optimum is said to be compacted "wet of optimum" whereas a soil compacted to a lower degree of saturation is said to be compacted "dry of optimum". As indicated in Figure 2, the Standard Proctor optimum water content of clayey soils is often close to their plastic limit, but the scatter is important. Fleureau et al. (2002) propose relationships between w_{opt} and the liquid limit of clayey soils, w_L; for the Standard Proctor optimum, the relationship is the following:

$$W_{opt} = 1.99 + 0.46\, w_L - 0.0012 w_L^2 \qquad (1)$$

Figure 3 compares the values of dry density and water content of clayey soils obtained at the optimum with the Standard and Modified Proctor tests.

The fabric of compacted soils has been widely studied, most often by mercury intrusion porosimetry. It has generally been observed that soils compacted on the dry side of optimum have a bimodal pore-size distribution whereas soils compacted on the wet side of optimum have a single family of pores (e.g., Ahmed et al., 1974; Delage et al., 1996; Vanapalli et al., 1999; Watabe et al., 2000). When prepared on the dry side, aggregates of particles are formed and, as indicated, for example, by the test results obtained by Delage et al. (1996) on Jossigny silt (Fig. 4), there are two families of pores: intra-aggregate pores or micropores (entrance pore radii of about 0.3 μm) and inter-aggregate pores or macropores (about 4 μm). On the wet side, the soil fabric appears more homogeneous with a single family of pores: micropores (about 0.5 μm for the Jossigny silt). The optimum thus forms a transition and can appear with one or two families of pores. The soil fabric is directly reflected in the Water Retention

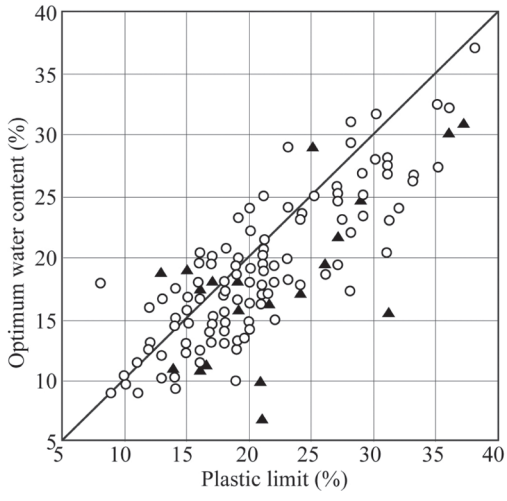

Figure 2. Correlation between Standard Proctor optimum water content and plastic limit. The black triangles correspond to the data used to produce Figure 8 (after Marinho & Olivera, 2012).

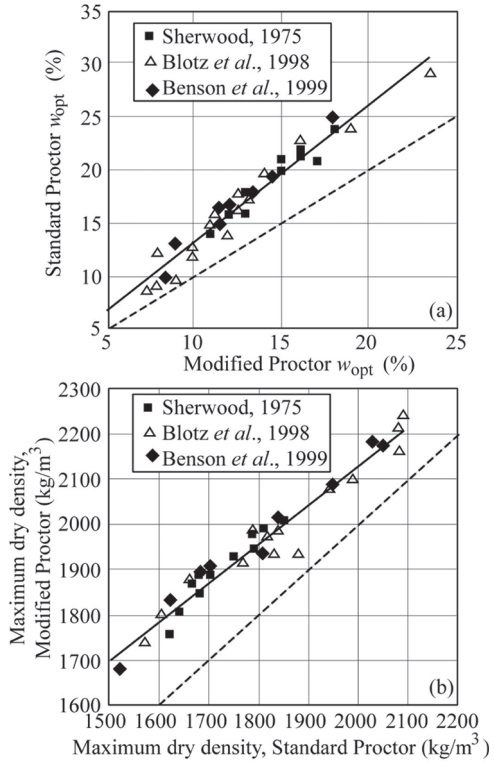

Figure 3. Correlations between the optimum water contents (a) and the maximum dry densities (b) of the Standard and Modified proctor compaction tests on clayey soils (after Chapuis, 2002).